

ESL-TR-87-61

## MODELING OF AIRCRAFT FIRE SUPPRESSION

DR. W.J. ENGLAND, E.T. MOREHOUSE JR,  
L.H. TEUSCHER, J. HERTEL, S.L. QUON,  
B.D. MCGILL

TRACER TECHNOLOGIES  
5820 OVERLIN DRIVE, SUITE 203  
SAN DIEGO CA 92121

OCTOBER 1988

FINAL REPORT

JULY 1986 - APRIL 1988

DTIC  
ELECTE  
OCT 30 1989  
S E D

APPROVED FOR PUBLIC RELEASE: DISTRIBUTION UNLIMITED



# AFESC

ENGINEERING & SERVICES LABORATORY  
AIR FORCE ENGINEERING & SERVICES CENTER  
TYNDALL AIR FORCE BASE, FLORIDA 32403

89 10 27 149

AD-A213 884

NOTICE

PLEASE DO NOT REQUEST COPIES OF THIS REPORT FROM  
HQ AFESC/RD (ENGINEERING AND SERVICES LABORATORY).

ADDITIONAL COPIES MAY BE PURCHASED FROM:

NATIONAL TECHNICAL INFORMATION SERVICE

5285 PORT ROYAL ROAD

SPRINGFIELD, VIRGINIA 22161

FEDERAL GOVERNMENT AGENCIES AND THEIR CONTRACTORS  
REGISTERED WITH DEFENSE TECHNICAL INFORMATION CENTER  
SHOULD DIRECT REQUESTS FOR COPIES OF THIS REPORT TO:

DEFENSE TECHNICAL INFORMATION CENTER

AMERON STATION

ALEXANDRIA, VIRGINIA 22314

NOTICE

PLEASE DO NOT REQUEST COPIES OF THIS REPORT FROM  
HQ AFESC/RD (ENGINEERING AND SERVICES LABORATORY).  
ADDITIONAL COPIES MAY BE PURCHASED FROM:

NATIONAL TECHNICAL INFORMATION SERVICE  
5285 PORT ROYAL ROAD  
SPRINGFIELD, VIRGINIA 22161

FEDERAL GOVERNMENT AGENCIES AND THEIR CONTRACTORS  
REGISTERED WITH DEFENSE TECHNICAL INFORMATION CENTER  
SHOULD DIRECT REQUESTS FOR COPIES OF THIS REPORT TO:

DEFENSE TECHNICAL INFORMATION CENTER  
CAMERON STATION  
ALEXANDRIA, VIRGINIA 22314

UNCLASSIFIED

SECURITY CLASSIFICATION OF THIS PAGE

REPORT DOCUMENTATION PAGE				Form Approved OMB No. 0704-0188	
1a. REPORT SECURITY CLASSIFICATION UNCLASSIFIED			1b. RESTRICTIVE MARKINGS		
2a. SECURITY CLASSIFICATION AUTHORITY			3. DISTRIBUTION / AVAILABILITY OF REPORT		
2b. DECLASSIFICATION / DOWNGRADING SCHEDULE			Approved for Public Release. Distribution Unlimited.		
4. PERFORMING ORGANIZATION REPORT NUMBER(S)			5. MONITORING ORGANIZATION REPORT NUMBER(S)		
			ESL-TR-87-61		
6a. NAME OF PERFORMING ORGANIZATION		6b. OFFICE SYMBOL (if applicable)	7a. NAME OF MONITORING ORGANIZATION		
Tracer Technologies			Air Force Engineering and Services Center		
6c. ADDRESS (City, State, and ZIP Code)			7b. ADDRESS (City, State, and ZIP Code)		
5820 Overlin Drive, Suite 203 San Diego CA 92121			HQ AFESC/RDCF Tyndall AFB FL 32403-6001		
8a. NAME OF FUNDING / SPONSORING ORGANIZATION		8b. OFFICE SYMBOL (if applicable)	9. PROCUREMENT INSTRUMENT IDENTIFICATION NUMBER		
HQ AFESC/RD			Contract #F08635-86-C-0366		
8c. ADDRESS (City, State, and ZIP Code)			10. SOURCE OF FUNDING NUMBERS		
Tyndall AFB FL 32403-6001			PROGRAM ELEMENT NO.	PROJECT NO.	TASK NO.
			62206F	2673	00
					WORK UNIT ACCESSION NO.
					44
11. TITLE (Include Security Classification)					
Modeling of Aircraft Fire Suppression					
12. PERSONAL AUTHOR(S) Dr. Walter J. England, Edward T. Morehouse, Jr., Lynn H. Teuscher, Joseph Hertel, Steven L. Quon, Brian D. McGill					
13a. TYPE OF REPORT		13b. TIME COVERED		14. DATE OF REPORT (Year, Month, Day)	
Final		FROM Jul 86 to Apr 88		October 1988	
				15. PAGE COUNT	
				78	
16. SUPPLEMENTARY NOTATION					
Availability of this report is specified on reverse of front cover.					
17. COSATI CODES			18. SUBJECT TERMS (Continue on reverse if necessary and identify by block number)		
FIELD	GROUP	SUB-GROUP	Fire Suppression, Firefighting Agent,		
06	07		Fire Control, Aqueous Film Forming Foam (AFFF),		
			Fire Area, Fire Modeling Aircraft Fires. (See)		
19. ABSTRACT (Continue on reverse if necessary and identify by block number)					
Modeling of aircraft fire suppression studies show that the theoretical equations/ parameters for scaling of the required quantities of fire extinguishing agent from small test fires to large scale actual crash fires is feasible. Modeling was based on the use of the firefighting agent Aqueous Film Forming Foam (AFFF) which the United States Air Force currently uses in response to aircraft fires. The Fire suppression model relates fire control time to variables in the fire area, agent application rates and agent properties. This report contains the analysis data for various fire configurations resulting in good correlation between the predictive models and the actual events studied. keywords:					
20. DISTRIBUTION / AVAILABILITY OF ABSTRACT			21. ABSTRACT SECURITY CLASSIFICATION		
<input type="checkbox"/> UNCLASSIFIED/UNLIMITED <input checked="" type="checkbox"/> SAME AS RPT. <input type="checkbox"/> DTIC USERS			unclassified		
22a. NAME OF RESPONSIBLE INDIVIDUAL			22b. TELEPHONE (Include Area Code)		22c. OFFICE SYMBOL
Capt E. Thomas Morehouse, Jr.			(904) 283-6194		RDCF

DD Form 1473, JUN 86

Previous editions are obsolete.

SECURITY CLASSIFICATION OF THIS PAGE

(The reverse of this page is blank.)

UNCLASSIFIED

## PROJECT SUMMARY

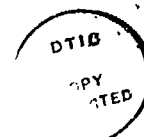
The overall purpose of the program was to validate and refine models that were developed in Phase I which related fire control time to the variables fire area, agent application rate, and agent properties. The models were based on the use of the firefighting agent Aqueous Film Forming Foam (AFFF) which the United States Air Force currently uses in response to aircraft ground fires. In particular, the Air Force was interested in the following types of fire configurations:

- One-dimensional fires, where the fire is limited to a fixed area fuel spill on the ground,
- One-dimensional crash fires with obstructions and heated objects within the fire,
- Three-dimensional crash fires, where fuel is continuously fed from an elevated source into an obstructed fire.

Data for the various parameters and fire configurations noted, was collected in a manner that greatly reduced the scatter common to previously published data sets.

The analysis of data for the various fire configurations resulted in a good correlation between the predictive models and the actual events being studied.

Accession For	
NTIS GRA&I	<input checked="checked" type="checkbox"/>
DTIC TAB	<input type="checkbox"/>
Unannounced	<input type="checkbox"/>
Justification	
By	
Distribution/	
Availability Codes	
Dist	Avail and/or Special
A-1	



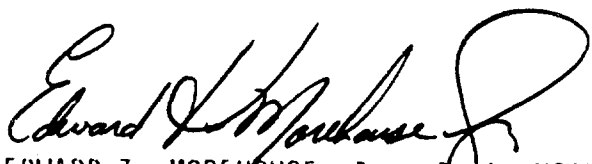
## PREFACE

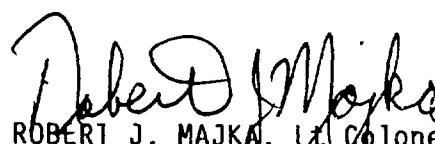
This technical report was prepared by Tracer Technologies, 5820 Overlin Drive, Suite 203, San Diego CA 92121, under Contract Number F08635-86-C-0366, for the Air Force Engineering and Services Center, Engineering and Services Laboratory (AFESC/RDCF), Tyndall Air Force Base, Florida 32403-6001.

Captain E. Thomas Morehouse Jr., was the project officers for HQ AFESC/RDCF. This report summarizes work accomplished between July 1986 and April 1988. This technical report was submitted as part of the Small Business Innovative Research (SBIR) Program and has been published according to SBIR Directives in the format in which it was submitted.


This report has been reviewed by the Public Affairs Office (PA) and is releasable to the National Technical Information Service (NTIS). At NTIS, it will be available to the general public, including foreign nationals.

This report has been reviewed and is approved for publication.

  
EDWARD T. MOREHOUSE, Jr., Capt, USAF  
Project Officer

  
ROBERT J. MAJKA, Lt Colonel, USAF  
Chief, Engineering Research  
Division

  
JOSEPH L. WALKER  
Chief, Fire Technology Branch

  
LAWRENCE D. HOKANSON, Colonel, USAF  
Director of Engineering and Services  
Laboratory

# TABLE OF CONTENTS

Section	Title	Page
I	INTRODUCTION.....	1
A.	Objective.....	1
B.	Background.....	2
C.	Scope.....	3
II	TASK DESCRIPTION.....	5
A.	TASK 1.....	7
B.	TASK 2.....	8
C.	TASK 3.....	9
D.	TASK 4.....	10
E.	TASK 5.....	11
F.	TASK 6.....	12
1.	Task 6A.....	12
2.	Task 6B.....	13
G.	TASK 7.....	14
III	DATA COLLECTION SYSTEM.....	15
A.	INSTRUMENTATION.....	15
1.	Radiometers.....	15
2.	Thermocouples.....	16
B.	DATA ACQUISITION.....	16
1.	Radiometer Flux Data.....	16
2.	AFFF Measurements.....	16
3.	Meteorological Data.....	20
4.	Fuel Flow Rates.....	20
5.	Thermocouple Data.....	21
6.	Test Chronicles.....	21
IV	TEST PROCEDURES AND METHODS.....	22
A.	EXPERIMENT TEAM.....	22
B.	TEST CONFIGURATION.....	22
1.	Task 1, 2 and 7 Test Configuration.....	24

TABLE OF CONTENTS  
(Continued)

Section	Title	Page
	2. Task 3 Test Configuration.....	24
	3. Task 4 Test Configuration.....	24
	4. Task 5 Test Configuration.....	24
	5. Task 6A Test Configuration.....	29
	6. Task 6B Test Configuration.....	29
	C. TEST PROCEDURE.....	33
	D. FIREFIGHTING PROCEDURE.....	33
V	THEORETICAL CONSIDERATIONS.....	35
	A. PHASE 1 SUMMARY.....	35
	B. TASK 5 OBSTACLE HEAT TRANSFER MODEL.....	36
	C. TASK 6 EXPANDING POOL MODEL.....	39
VI	DATA ANALYSIS.....	41
	A. DETERMINATION OF CONTROL TIME FROM RADIOMETER DATA.....	41
	1. Determination of 10 Percent Value of Heat Flux.....	41
	2. Control Time Selection.....	42
	B. STATISTICAL ANALYSIS.....	43
VII	DATA PRESENTATION.....	45
	A. EFFECT OF POOL AREA ON BURN RATE.....	45
	B. CONTROL TIME VS APPLICATION RATE.....	45
	C. EFFECT OF WINDSPEED ON CONTROL TIME.....	48
	D. EFFECT OF FOAM EXPANSION RATIO ON CONTROL TIME.....	56
	E. EFFECT OF TWO-POINT ATTACKS ON CONTROL TIMES.....	56

TABLE OF CONTENTS  
(Concluded)

Section	Title	Page
VIII	MODEL RESULTS.....	58
A.	TASK 1 RESULTS.....	58
B.	TASK 2 RESULTS.....	58
C.	RESULTS OF COMBINED TASK 1, 2 AND 7 DATA.....	60
D.	TASK 3 RESULTS.....	60
	1. Task 3 Foam Flow Model Results.....	60
E.	TASK 4 RESULTS.....	61
F.	TASK 5 RESULTS.....	63
	1. AFFF Effectiveness In Preventing Reignition.....	63
	2. Task 4 and 5 Foam Flow Model Results.....	67
G.	TASK 6A RESULTS.....	69
	1. Task 6A Equivalent Foam Flow Model Results.....	69
H.	TASK 6B RESULTS.....	71
I.	COMPREHENSIVE MODEL.....	72
IX	CONCLUSIONS AND RECOMMENDATIONS.....	74
A.	CONCLUSIONS.....	74
B.	RECOMMENDATIONS.....	75
APPENDIX		
A	EQUIVALENT FOAM FLOW RATES FOR TWO-DIMENSIONAL MODELS.....	76

## LIST OF FIGURES

Figure	Title	Page
1	Data Capture Configuration.....	17
2	Task 7 Test 2 Radiometer Outputs.....	18
3	Fire Pit Configuration.....	23
4	Task 1, 2 and 7 Test Configuration.....	25
5	Task 3 Test Configuration.....	26
6	Task 4 Test Configuration.....	27
7	Task 5 Test Configuration.....	28
8	Task 5 Thermocouple Configuration.....	30
9	Task 6A Test Configuration.....	31
10	Task 6B Test Configuration.....	32
11	Thermal Mass Heat Transfer Simulation.....	38
12	Pool Radius vs Time for Expanding Pool Fire.....	40
13	Burn Rate vs Pool Size.....	46
14	Task 1 Data.....	47
15	Task 2 Data.....	49
16	Task 3 Data.....	50
17	Task 4 and 5 Data.....	51
18	Task 6A Data.....	52
19	Task 6B Data.....	53
20	Tasks 1, 2, 3, and 7 Data.....	54
21	Effects of Wind Speed on Control Time.....	55

LIST OF FIGURES  
(Concluded)

Figure	Title	Page
22	Foam Expansion vs Control Time.....	57
23	Task 3 Foam Flow Model.....	62
24	Obstacle Temperature Profile.....	66
25	Task 4 and Task 5 Foam Flow Model.....	68
26	Equal Area Circle and Sector.....	70
27	Estimated Control Time vs Actual Control Time.....	73
A-1	Equivalent Foam Flow vs Actual Foam Flow.....	77

# LIST OF TABLES

Table	Title	Page
1	PHASE II TASK DESCRIPTION MATRIX.....	6
2	TASK 1 TEST MATRIX.....	7
3	TASK 2 TEST MATRIX.....	8
4	TASK 3 TEST MATRIX.....	9
5	TASK 4 TEST MATRIX.....	10
6	TASK 5 TEST MATRIX.....	11
7	TASK 6A TEST MATRIX.....	12
8	TASK 6B TEST MATRIX.....	13
9	TASK 7 TEST MATRIX.....	14
10	SUMMARY OF MODEL EQUATIONS AND THEIR REGRESSION RESULTS.....	59
11	MAXIMUM TEMPERATURES AT EACH LOCATION FOLLOWING SUPPRESSION.....	65

## SECTION I

### INTRODUCTION

#### A. OBJECTIVE

In responding to aircraft ground fires, the United States Air Force presently uses Aqueous Film Forming Foam (AFFF) as a primary fire suppression and control agent.

The time to control or extinguish a fire with a specific agent is a function of a number of variables such as the type of fuel, the properties of the agent, the area of the fire, and the extinguishant application rate. However, control time is also a function of less definable variables such as the weather conditions, the presence or absence of obstructions, and heated metal components within the fire. For aircraft ground fires, three fire configurations are of particular concern to the Air Force:

- One-dimensional fires, where the fire is limited to a fixed area fuel spill on the ground,
- One-dimensional crash fires with obstructions and heated objects within the fire,
- Three-dimensional crash fires, where fuel is continuously fed from an elevated source into an obstructed fire.

The overall objective of the program was to develop and validate models which related fire control time to the important variables noted. During Phase I of the study, several models were developed based upon theoretical considerations and data found in the literature. To completely accomplish this goal, however, there were several specific additional objectives that had to be met. These were:

1. Design and conduct a set of experimental methods that minimized the prediction errors associated with the derived expressions.
2. Determine the impact on fire suppression times of various obstacles (simulated aircraft parts) that were placed in the pool fire.
3. Determine the effect on control time of a two-dimensional expanding pool fire with a continuous fuel source.

4. Determine the effect on control time of a three-dimensional pool fire with a continuous fuel flow from a simulated aircraft wing i.e., a pool fire under an aircraft with a "continuous" fuel source from the tanks.
5. Determine if derived predictive expressions developed from small- and medium-scale fires could be applied toward large-scale fires.

## B. BACKGROUND

During Phase I of a study to examine these issues, Tracer Technologies searched over 130 articles and reports to: (1) determine if prior models of fire suppression had been developed and (2) to compile data from which to derive a theoretically based, empirically validated model of pool fire suppression.

In Phase I two applicable fire/extinguishant combinations were modeled. These combinations were:

- Aircraft fuel spill fire without the presence of obstacles using AFFF, and
- Aircraft fuel spill fire with obstacles using AFFF.

The study used data from small- and medium-scale fire extinguishment tests to develop fire control models for the two configurations. Theoretical considerations were used as a basis for much of the analysis. Statistical approaches (regression analysis) were used to develop the final relationships. The result was an analytical expression for determining the time to control (or total quantity of AFFF needed) as a function of the foam flow rate per unit area, and the area of the fire.

The model derived in Phase I was

$$t = k (A^{2/7} / F^{4/7})$$

where     $t$  = Control Time (sec)  
            $A$  = Pool Area (ft<sup>2</sup>)  
            $k$  = Empirically Derived Constant  
            $F$  = Foam Application Rate (gpm/ft<sup>2</sup>)

The Phase 1 results indicated that there was a basis for a fire-suppression model but there was a significant amount of scatter in the data. This was felt to be due to the inconsistent manner in which control times were measured by the many different investigators (198 data sets were used). In order to assure that

the models could be applied with a reasonable certainty, it was determined that a set of data should be obtained which was consistent in terms of measurement technique and definition of parameters.

### C. SCOPE

To eliminate the inconsistencies found in previously published data sets, data obtained under tightly controlled conditions was used to validate and refine the model developed in Phase I. To do this, a method to determine, in a consistent manner, the point at which a fire was controlled during the suppression effort was needed. This was accomplished through the use of radiometers which were capable of directly measuring the heat flux of the fire during each test. Using these measurements and defining a controlled fire as having 10 percent of the maximum heat flux of the uncontrolled fire, the control time was consistently determined. Scatter from data obtained in this manner was expected to be significantly smaller when compared to that associated with the widely published data used in Phase I.

Additionally, it was felt that further theoretical and experimental studies should be initiated to extend the predictive model to include obstacles present in fires. This data was obtained by placing various types of obstacles in the pool fires and observing their effects on control time. Three basic types of obstacles were included in the studies: (1) obstacles that did not have foam suppression blocking or thermal mass characteristics, (2) obstacles that were capable of blocking suppression efforts but had no thermal mass, (3) obstacles that had both suppression blocking and thermal mass properties.

In order to address the third and fourth objectives noted, data was collected to include the effects on control time of two- and three-dimensional continuous fuel source fires. A continuous fuel source fire was defined as being a fire that has a continuous source of fuel and was, therefore, unable to extinguish itself by consuming all of its fuel supply. The two-dimensional fire consisted of an expanding pool fire with the continuous fuel source at the pool center. The three-dimensional pool fire was configured such that fuel flowed continuously from an elevated source (simulated aircraft wing) and formed an expanding pool at the base of the simulated aircraft part.

To answer the fifth and final objective, data was collected over a range of pool sizes (100 ft<sup>2</sup> to 4418 ft<sup>2</sup>). This assumed that the model developed was capable of predicting control times over a large range of fire sizes.

Upon completion of the experimental portion of the study, the models were modified and extended from those initially established in Phase I to specifically address the objectives outlined. Significant improvements in the errors associated with application of the models was achieved.

## SECTION II

### TASK DESCRIPTION

A series of experiments was designed to examine the relationship between control time, foam application rate, and fire area. A number of fuel and foam physical parameters had been included in the original development of the model and produced only second-order effects in the control time. The effect of wind speed on control time was examined during Phase II. It was found it also produced a second-order effect as long as foam throw distance was not significantly reduced. Once these relationships were known, further tests were conducted to examine what effects simulated aircraft parts in the fire had on control time. A series of experiments was also conducted with two-dimensional and three-dimensional fires to see how well the refined Phase I model applied to these scenarios.

Experimentation was broken down into seven tasks outlined in Table 1. In Tasks 1, 2, and 7, burn rate, control time, foam application rate, pool area data, and foam parameter data, were gathered so that the model could be validated and refined. In Tasks 3, 4, and 5 the effects of various types of simulated aircraft parts on control time were examined. In Task 6, two- and three-dimensional fires on control time were examined to see if the basic model could be applied to these types of fires. Each task will be described in detail in the following paragraphs.

TABLE 1. PHASE II TASK DESCRIPTION MATRIX

TASK #	TASK DESCRIPTION	TOTAL TESTS CONDUCTED
1	Investigate Foam Parameters Burn Rate Tests	18
2	Model Validation-Area/Application Rate Burn Rate Tests	15
3	Effects of Simulated Aircraft Parts	21
4	Model Validation-Simulated Aircraft Parts	22
5	Model Validation-Simulated Aircraft Parts	8
6A	Two-Dimensional-Model Development	13
6B	Three-Dimensional-Model Development	19
7	Testing With Full-Scale Fires	3

# A. TASK 1

The objective of Task 1 was to examine the relationship of various foam application rates on control time while holding the pool area constant at 100 ft<sup>2</sup>. Before beginning these tests, experimental burns were conducted to determine accurate burn rates for the pool configurations used. The burnoff rate was required to accurately predict the amount of fuel to be used in each test to avoid premature fire extinguishment due to a lack of fuel. The various foam application rates used in each of the tasks were expressed in the units of gallons per minute per square foot of pool area (gal/ft<sup>2</sup>-min). Table 2 outlines the parameters of the various tests that were accomplished in Task 1.

TABLE 2. TASK 1 TEST MATRIX

TASK #	TEST #	POOL AREA (ft <sup>2</sup> )	FOAM APPLICATION (gal/ft <sup>2</sup> -min)
1	1	100.00	burnrate
1	2	100.00	burnrate
1	3	100.00	0.0250
1	4	100.00	0.0500
1	5	100.00	0.1000
1	6	100.00	0.1500
1	7	100.00	0.2000
1	8	100.00	0.0250
1	9	100.00	0.0500
1	10	100.00	0.1000
1	11	100.00	0.1500
1	12	100.00	0.2000
1	13	100.00	0.0375
1	14	100.00	0.0310
1	15	100.00	0.0375
1	16	100.00	0.0310
1	17	100.00	0.0250
1	18	100.00	0.0250

## B. TASK 2

The objective of Task 2 was to investigate the relationship between pool area and control time while keeping the foam application rate to pool area ratio constant. Also, a two-point rather than a single-point attack was used for certain tests to determine if this affected control time. Table 3 summarizes the various foam flow rates and pool areas used in Task 2 testing.

TABLE 3. TASK 2 TEST MATRIX

TASK #	TEST #	POOL AREA (ft <sup>2</sup> )	FOAM APPLICATION (gal/ft <sup>2</sup> -min)	ATTACK POINTS
2	1	300.00	burnrate	-
2	2	300.00	0.100	1
2	3	300.00	0.100	1
2	4	300.00	0.100	2
2	5	300.00	0.100	2
2	6	600.00	0.100	1
2	7	600.00	0.100	2
2	8	600.00	0.050	1
2	9	300.00	0.050	1
2	10	300.00	0.025	1
2	11	600.00	burnrate	-
2	12	600.00	0.050	1
2	13	600.00	0.050	1
2	14	300.00	0.050	2
2	15	300.00	0.025	2

### C. TASK 3

Task 3 was conducted to determine the area effects of simulated aircraft parts present within a pool fire, without considering the effects of their blocking of fire suppression efforts or of their thermal masses. This task was accomplished by placing a thin circular ring in the center of the pool before fuel application. This ring was tall enough to block fuel from entering the center of the pool but not so tall as to impede foam application. The experiment, thus, consists of two concentric rings, with the fire burning in the annulus and a nonflammable area at the center of the pool ( See Section IV). The maximum size of the internal ring for a given outer ring size was constrained by restricting the difference in radii between the two rings to the thickness that renders the fire optically thick (See Section V). The ratio of inner to outer areas ranged from 5 percent to 50 percent. Table 4 outlines the experiments conducted.

TABLE 4. TASK 3 TEST MATRIX

TASK #	TEST #	OUTER AREA (ft <sup>2</sup> )	INNER AREA (ft <sup>2</sup> )	FOAM APPLICATION (gal/ft <sup>2</sup> -min)
3	1	150.00	15.0	0.1000
3	2	300.00	15.0	0.0500
3	3	150.00	50.0	0.1000
3	4	300.00	50.0	0.0500
3	5	600.00	50.0	0.0500
3	6	300.00	150.0	0.0500
3	7	600.00	150.0	0.0375
3	8	150.00	15.0	0.2000
3	9	300.00	15.0	0.1500
3	10	150.00	50.0	0.2000
3	11	300.00	50.0	0.1250
3	12	600.00	50.0	0.1500
3	13	300.00	150.0	0.1000
3	14	600.00	150.0	0.1000
3	15	300.00	50.0	0.0500
3	16	300.00	15.0	0.0500
3	17	300.00	150.0	0.0500
3	18	150.00	15.0	0.2000
3	19	300.00	50.0	0.0500
3	20	300.00	100.0	0.0500
3	21	100.00	000.0	0.1500

#### D. TASK 4

Task 4 consisted of an investigation of the relationship between control time, pool area, and foam application rate with obstacles capable of blocking suppression efforts placed within the pool area. The obstacles, placed in the center of the pool, were circular metal arcs of varying radius (See Section IV). With the exception of a 1000 ft<sup>2</sup> fire, the application rates, pool areas and suppressor locations in this task, were identical to those found in Task 3 testing. This allows a direct comparison of the two tasks. An Air Force P-4 Fire Truck was used to suppress the 1000 ft<sup>2</sup>-fire in this task. The results of this test were compared with the Task 2, Test 11 results to determine obstacle effects involved with the use of a Fire Truck. The various test parameters of Task 4 are outlined in Table 5.

TABLE 5. TASK 4 TEST MATRIX

TASK #	TEST #	OUTER AREA (ft <sup>2</sup> )	INNER RADIUS (ft <sup>2</sup> )	FOAM APPLICATION (gal/ft <sup>2</sup> -min)
4	1	150.00	2.18	0.100
4	2	300.00	2.18	0.050
4	3	150.00	3.99	0.100
4	4	300.00	3.99	0.050
4	5	600.00	3.99	0.050
4	6	300.00	6.91	0.050
4	7	600.00	6.91	0.050
4	8	150.00	2.18	0.200
4	9	300.00	2.18	0.150
4	10	150.00	3.99	0.200
4	11	300.00	3.99	0.150
4	12	600.00	3.99	0.150
4	13	300.00	6.91	0.150
4	14	600.00	6.91	0.150
4	15	1000.00	6.91	0.150
4	16	600.00	6.91	0.200
4	17	600.00	3.99	0.150
4	18	600.00	2.18	0.050
4	19	300.00	2.18	0.050
4	20	600.00	0.00	0.100
4	21	1000.00	0.00	0.150
4	22	300.00	0.00	0.050

# E. TASK 5

The objective of Task 5 was to study the effect of the presence of an obstacle of significant thermal mass on the effectiveness of AFFF in controlling a JP-4 fire and preventing its reignition. The object, which was the same configuration as the obstacles found in Task 4, would be constructed from either a mild steel or aluminum material of varying thicknesses and would absorb and retain sensible heat during a preburn and a portion of the suppression period (See Section V). During suppression, the surface of the object would cool down as foam was applied to the surface. The surface temperature, however, could rise again above the ignition temperature of the fuel after the fire had been controlled or extinguished due to heat transfer from the interior of the object to its surface. Thus, fuel vapor could reignite. Table 6 outlines the tests conducted in this task. The pool area of all Task 5 tests was held constant at 150 ft<sup>2</sup>. To determine the effect of the thermally thick object on fire control time, the data was compared directly to that of the 150 ft<sup>2</sup> tests of Task 4.

To monitor the temperature of the obstacle during the test, thermocouples were placed on its surface and interior. Thermocouple data acquisition is discussed in Section III while test configuration and thermocouple placement is detailed in Section V.

TABLE 6. TASK 5 TEST MATRIX

TASK #	TEST #	FOAM APPLICATION (gal/ft <sup>2</sup> -min)	THICKNESS (in)	PREBURN (sec)	OBSTACLE MATERIAL
5	1	.05	1/4	120	Steel
5	2	.15	1/4	120	Steel
5	3	.05	1/2	60	Steel
5	4	.15	1/2	60	Steel
5	5	.05	1/2	120	Steel
5	6	.15	1/2	120	Steel
5	7	.05	1/4	120	Aluminum
5	8	.15	1/4	120	Aluminum

## F. TASK 6

Task 6 was used to examine the applicability of the developed model on two- and three-dimensional fires. A two-dimensional fire is defined as one with an expanding radius due to the presence of a fuel source. A three-dimensional fire implies fuel flowing in the vertical dimension, as well as expanding horizontally.

### 1. Task 6A

The two-dimensional fire was achieved by allowing fuel to spread radially over a horizontal surface. The fuel source was located at the pool center at ground level. Following ignition, the pool would continue to expand until the rate at which the fuel is consumed is equal to the input fuel rate. Section V discusses the methods used to determine the equilibrium pool area. Control was attempted when the steady-state condition was achieved. The rate of foam application, the fuel flow rate, and the preburn time were varied to determine their respective effects on control time. Control was not considered possible if it was not achieved before the burning pool reached the slab edge. Table 7 outlines the various test parameters found in Task 6A testing. A description of the Task 6A test configuration is found in Section IV.

TABLE 7. TASK 6A TEST MATRIX

TASK #	TEST #	FOAM APPLICATION (gal/ft <sup>2</sup> -min)	FUEL FLOW (gal/min)	PREBURN (sec)
6A	1	0.15	5	30
6A	2	0.15	10	120
6A	3	0.05	15	30
6A	4	0.05	15	30
6A	5	0.15	15	30
6A	6	0.25	15	60
6A	7	0.30	15	90
6A	8	0.20	10	90
6A	9	0.05	15	90
6A	10	0.05	15	30
6A	11	0.25	15	90
6A	12	0.15	5	30
6A	13	0.10	15	30

## 2. Task 6B

The three-dimensional fire was achieved when fuel was allowed to flow down and off of the sides of an inclined ramp and spread radially on a flat horizontal surface at the bottom of the ramp. As in Task 6A, the burning fuel will continue to expand until the rate at which fuel is burned will equal to the input flow rate. Suppression began once this equilibrium was achieved. In Section IV, the test configuration and the methods that were used to determine the equilibrium pool area are discussed. Table 2 outlines the various testing conducted in this Task.

TABLE 2. TASK 6B TEST MATRIX

TASK #	TEST #	FOAM APPLICATION (gal/ft <sup>2</sup> -min)	FUEL FLOW (gal/min)	PREBURN (sec)
6B	1	1.618	5	30
6B	2	0.746	15	30
6B	3	0.722	15	30
6B	4	0.677	15	90
6B	5	0.707	15	120
6B	6	0.692	15	60
6B	7	1.131	10	30
6B	8	0.737	15	150
6B	9	0.760	15	60
6B	10	0.932	10	30
6B	11	10.645	5	30
6B	12	0.517	10	30
6B	13	0.446	15	30
6B	14	0.421	15	30
6B	15	0.967	15	30
6B	16	0.414	15	90
6B	17	0.704	15	90
6B	18	1.053	15	90
6B	19	0.683	10	30

G. TASK 7.

The object of Task 7 was to determine if the model, developed using data for relatively small fires, was applicable to larger configurations. The pool area utilized was 4418 ft<sup>2</sup> and suppression was achieved using an Air Force P-19 Fire Truck. A summary of the Task 7 tests is shown in Table 9.

TABLE 9. TASK 7 TEST MATRIX

TASK #	TEST #	POOL AREA (ft <sup>2</sup> )	FOAM APPLICATION (gal/ft <sup>2</sup> -min)
7	1	4418	0.05
7	2	4418	0.10
7	3	4418	0.20

## SECTION III

### DATA COLLECTION SYSTEM

This section describes the instrumentation and methodology used in collecting the relevant data. The relevant data collected for these tests included that associated with meteorological conditions, AFFF application rate and properties, fuel consumed, the relative radiant flux of the flame over time, temperature of the obstacles, videotape of each experiment, and visual observations during each test.

#### A. INSTRUMENTATION

##### 1. Radiometers

Much of the uncertainty in previous suppression data arose from the methods used to determine the point of fire control. A few of the experiments used radiometers while most visually determined the point at which the fire was controlled. A method as subjective as visually determining control times will not be consistent from test to test. To reduce this error, we measured the radiant flux from the fire at several locations around its perimeter. After steady-state was reached, suppression was initiated. When the radiant flux reached a level that was 10 percent of the recorded maximum steady-state value, the fire was considered under control.

The radiant flux was measured, using four radiometers. The radiometers, manufactured by Medtherm, each had a 150 degree angle of view. The radiometers were calibrated to yield approximately 0.25 BTU/ft<sup>2</sup>-sec per millivolt.

Because the radiometer signal varies linearly with the heat flux of the fire, placement of the radiometers in relation to the fire is crucial. The radiometers had to be placed close enough to the fire to yield reasonable signals, yet far enough away so that they would not burn. Attempts were also made to spread the radiometers as far apart as possible, under these constraints, to remove questions about measurement relative to the fire and suppression points of attack. This assumed that radiometer signals were indicative of the heat flux at different points around the fire and independent of each other. By comparing the signals, it was possible to more consistently estimate control time.

## 2. Thermocouples

In Task 5, barriers with thermal mass were placed in the fires as obstacles to determine whether thermally thick objects would reignite a pool of foam-covered JP-4. Thermocouples were placed on and in the barrier to monitor the temperature distribution of the barrier during heating and cooling. The locations of the various thermocouples are shown in Figure 8. The thermocouples were Type K thermocouples rated to 2000 degrees Centigrade.

## B. DATA ACQUISITION

### 1. Radiometer Flux Data

The radiometer signals were sampled at a sufficiently rapid rate to obtain an accurate measure of control time. A sample rate of 2 HZ was determined to be appropriate. With a sampling rate of 2 HZ and an average test duration of 2 minutes, 960 data records were recorded for each test. To reduce data collection problems and to speed up analysis, data from the radiometers was collected on both a microcomputer and a strip-chart recorder via a Metrabyte Dash 8 data-logger. The digital data was stored on both floppy disks and computer hard drive. This enabled quick easy access to the data during testing. A diagram of the radiometer data collection system is shown in Figure 1. During each test, a real-time graph of the radiometer signals was charted on the computer monitor. A sample graph is shown in Figure 2.

### 2. AFFF Measurements

The AFFF was 3 percent concentrate, manufactured to military specification by the ANSUL company. Refractometer readings were taken after each truckload of the 3 percent solution was made. Measurements of expansion ratios and drainage times were conducted for each solution and each time a different application nozzle was used.

The foam samples analyzed were collected by spraying the foam into a collector for AFFF. This specialized apparatus collects the foam sprayed from the nozzle and lets it drain into a graduated cylinder. The rate at which the liquid drops out

# RADIOMETER DATA CAPTURE

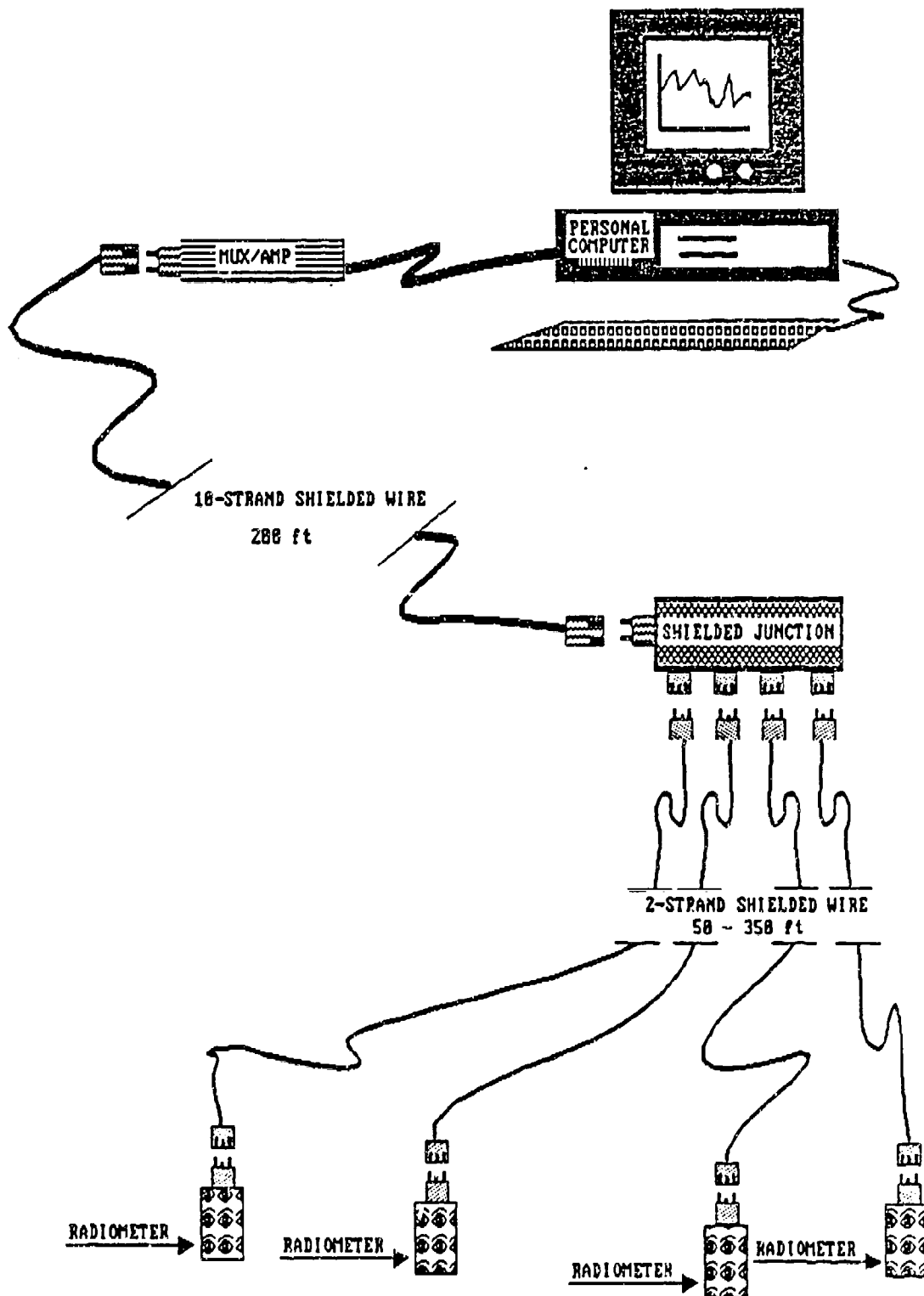


Figure 1. Data Capture Configuration

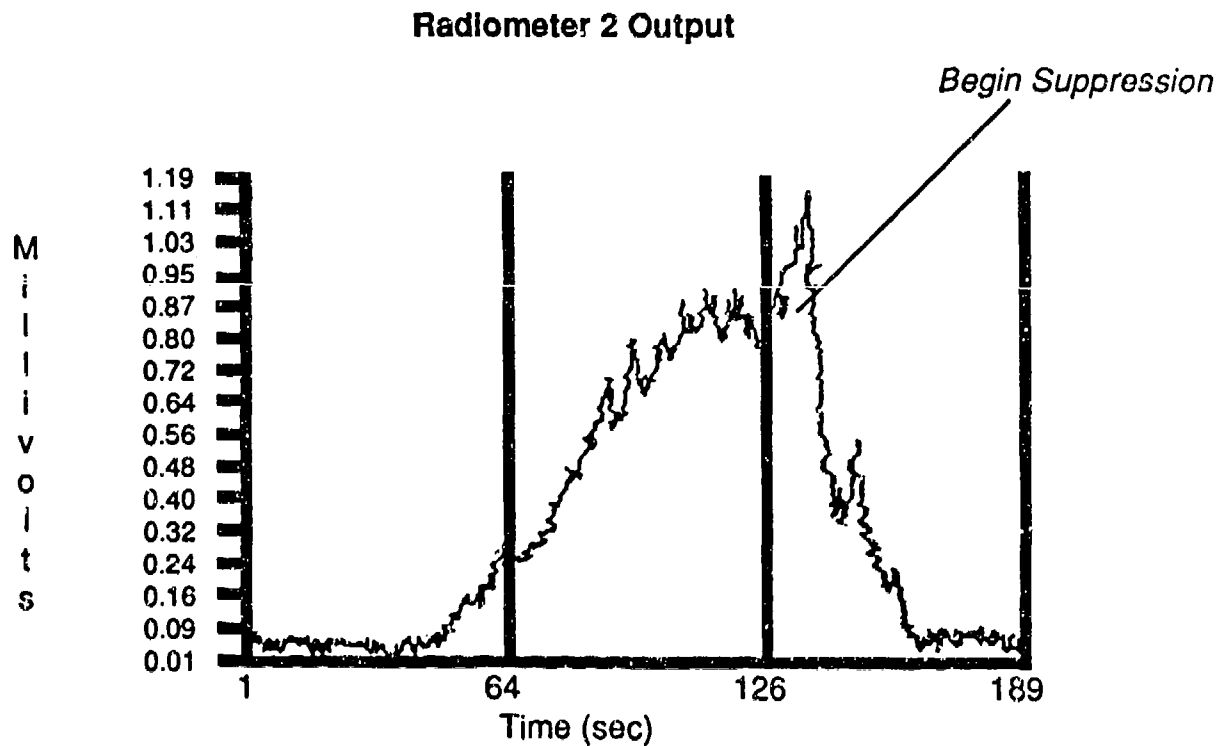
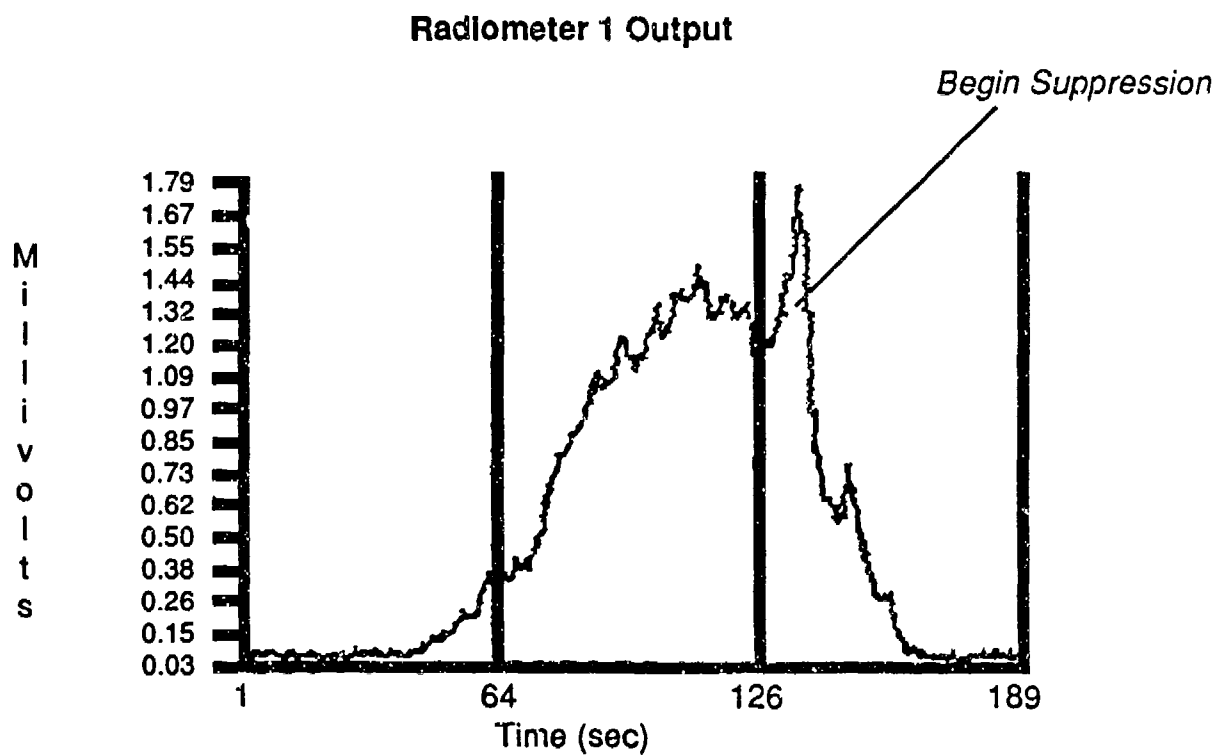


Figure 2. Task 7, Test 2 Radiometer Outputs

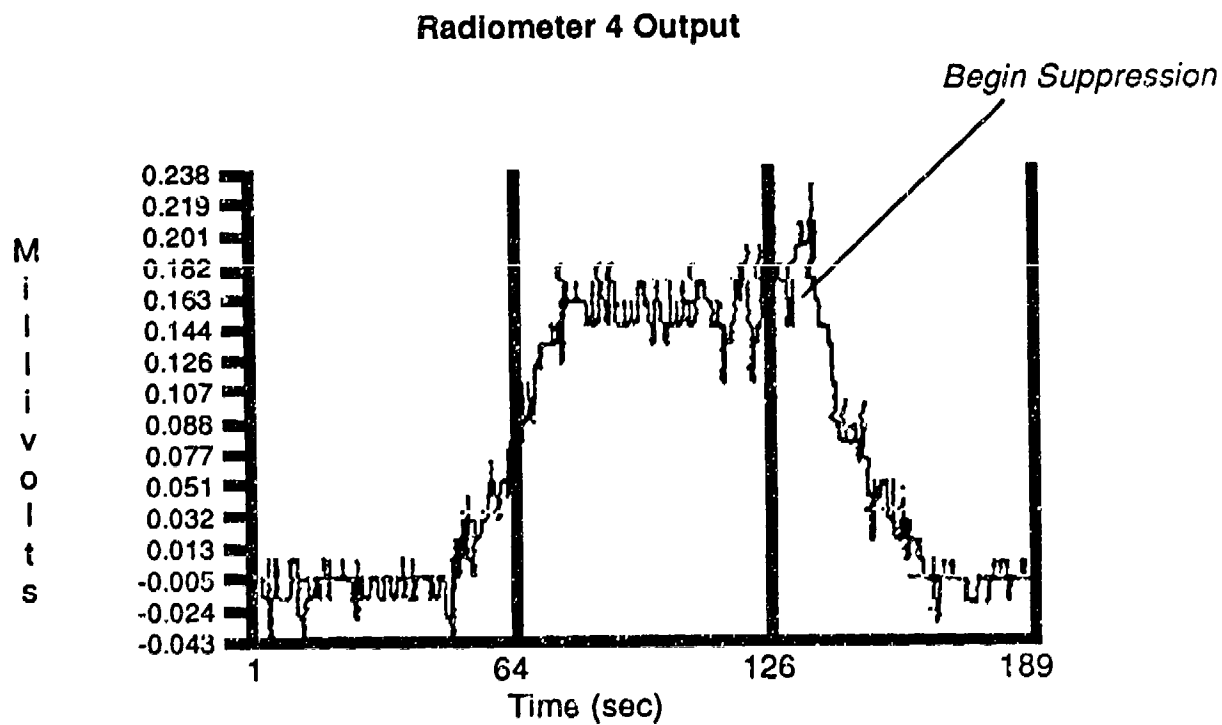
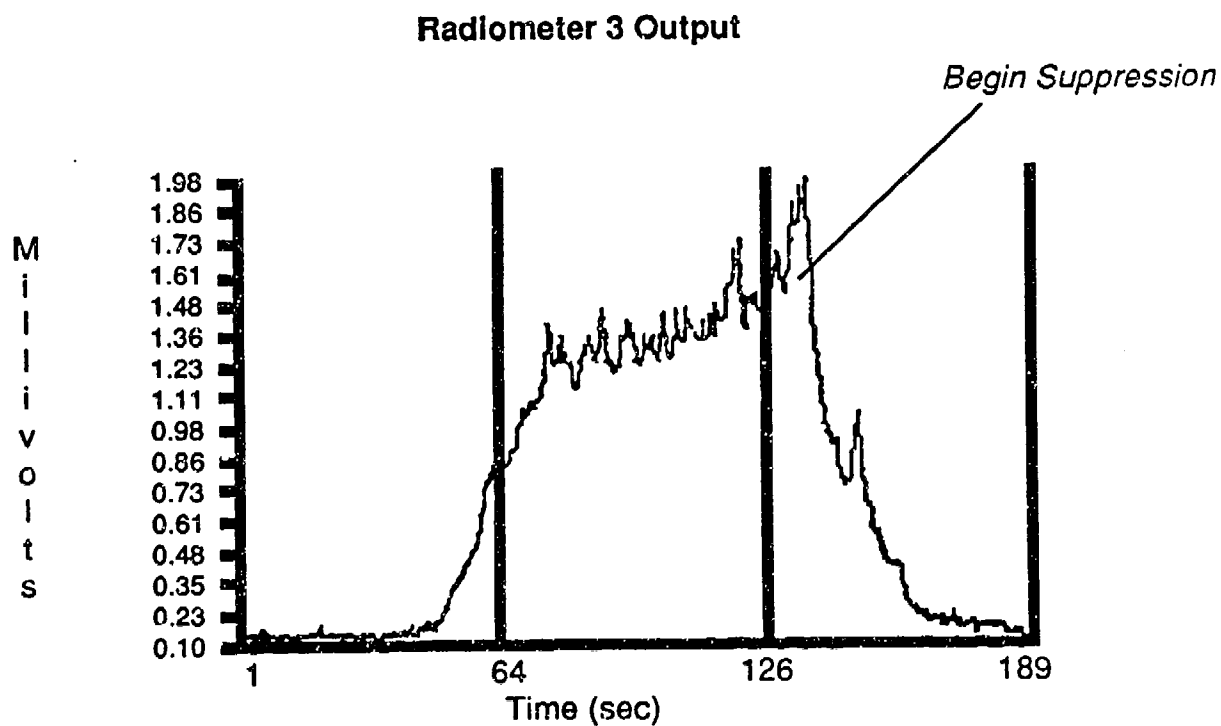


Figure 2. Task 7, Test 2 Radiometer Outputs (Concluded)

from the foam mass is called the drainage rate, which is a direct indication of degree and stability and the viscosity of the foam. A single value used to express the relative drainage times of different foams is the 25 percent drainage time; this is the time that it takes for 25 percent of the total liquid contained in the foam in the graduated cylinders to drain out. After the sample was collected in the graduated cylinder, a stopwatch was used to note the time at which the liquid level was visible at 25 percent of the volume of the cylinder.

After the drainage time was determined, the graduated cylinder was weighed twice; once with the foam sample and once with it completely empty. The expansion of the foam, or the expansion ratio was then calculated with the following equation:

$$\text{Expansion} = 1400 \text{ mL} / (\text{full weight of graduated cylinder minus empty weight (grams)})$$

These measurements are in accordance with National Fire Protection Association (NFPA) procedures.

Foam application rates were measured with in-line liquid flowmeters and readings were taken during foam application. The amount of foam used in each test was recorded with a totalizer as an alternative method to measure the application rate.

For tests conducted using trucks, the application rate was determined by: (1) measuring the volume of foam in the truck before and after each test and (2) through the water pump rated capacity of the truck.

### 3. Meteorological Data

Meteorological measurements included windspeed and direction which were both measured with hand-held anemometers. Readings were taken before and after each test burn (approximately 2 minutes apart) and the reported data is an average of the separate readings.

### 4. Fuel Flow Rates

For Task 6, fuel was continuously fed into the pool. The flow rates were measured with a flowmeter and a totalizer was used to double-check the flowmeter readings. For Tasks 1, 2, 3, 4, 5, and 7 the amounts of fuel used for each test were measured with a totalizer.

## 5. Thermocouple Data

The six thermocouple readings monitored in Task 5 were sampled at a rate of 2 Hz through a Hewlett-Packard data logger. The thermocouple data was printed in real-time and was stored on floppy disks for future use. The time of suppression initiation was marked in the data files as the tests took place to facilitate data interpretation.

## 6. Test Chronicles

All tests were recorded on videotape for future reference. Data sheets were used to record the data. In addition to the previously mentioned data, additional data were recorded. The radiometer locations were noted and sketched for each test and visually determined control times were recorded with a stopwatch.

## SECTION IV

### TEST PROCEDURES AND METHODS

#### A. EXPERIMENT TEAM

To maximize the probability of achieving the Phase II objectives, the expertise of the Phase I technical team was combined with that of the New Mexico Engineering Research Institute (NMERI) to design and conduct the experimental program at Tyndall AFB, Panama City, Florida. The use of this team assured continuity with the Phase I program and added the technical expertise of NMERI associated with designing and conducting fire suppression experimental programs.

#### B. TEST CONFIGURATION

All tests were conducted at two fire pits, of 1200 ft<sup>2</sup> and 4418 ft<sup>2</sup> areas, located at the fire training facility at Tyndall AFB, Florida. As Figure 3 illustrates, the 1200 ft<sup>2</sup> pool has the shape of a shallow inverted cone and allows tests of all surface areas up to the 1200 ft<sup>2</sup> area to be conducted. Testing for Tasks 1 through 6 took place in this 1200 ft<sup>2</sup> pool. The Task 7 testing took place in a 4418 ft<sup>2</sup> pool.

In Tasks 1, 2, 3, 4, 5 thin steel rings were used to contain the pools. Each of these rings was measured before testing to verify the areas that they contained. In Task 7 sand was used to contain the pool. Water was added until the water line reached the outlining ring. Fuel was then added until there was an approximately half-inch thick layer floating on the underlying water.

In Task 6, a mixture of sand and water was used to level off the pool area. The water was added so the fuel would not seep through the sand but would flow laterally across the surface. The pool areas of Task 6 were harder to determine, since they were continuous-source fires which resulted in pools that expanded until the growth rate of the pool was equal to the fuel burn-rate. A liquid spill model was developed to calculate the equilibrium pool area (See Section V). Visual estimates of the equilibrium pool area were recorded to verify the results of the model.

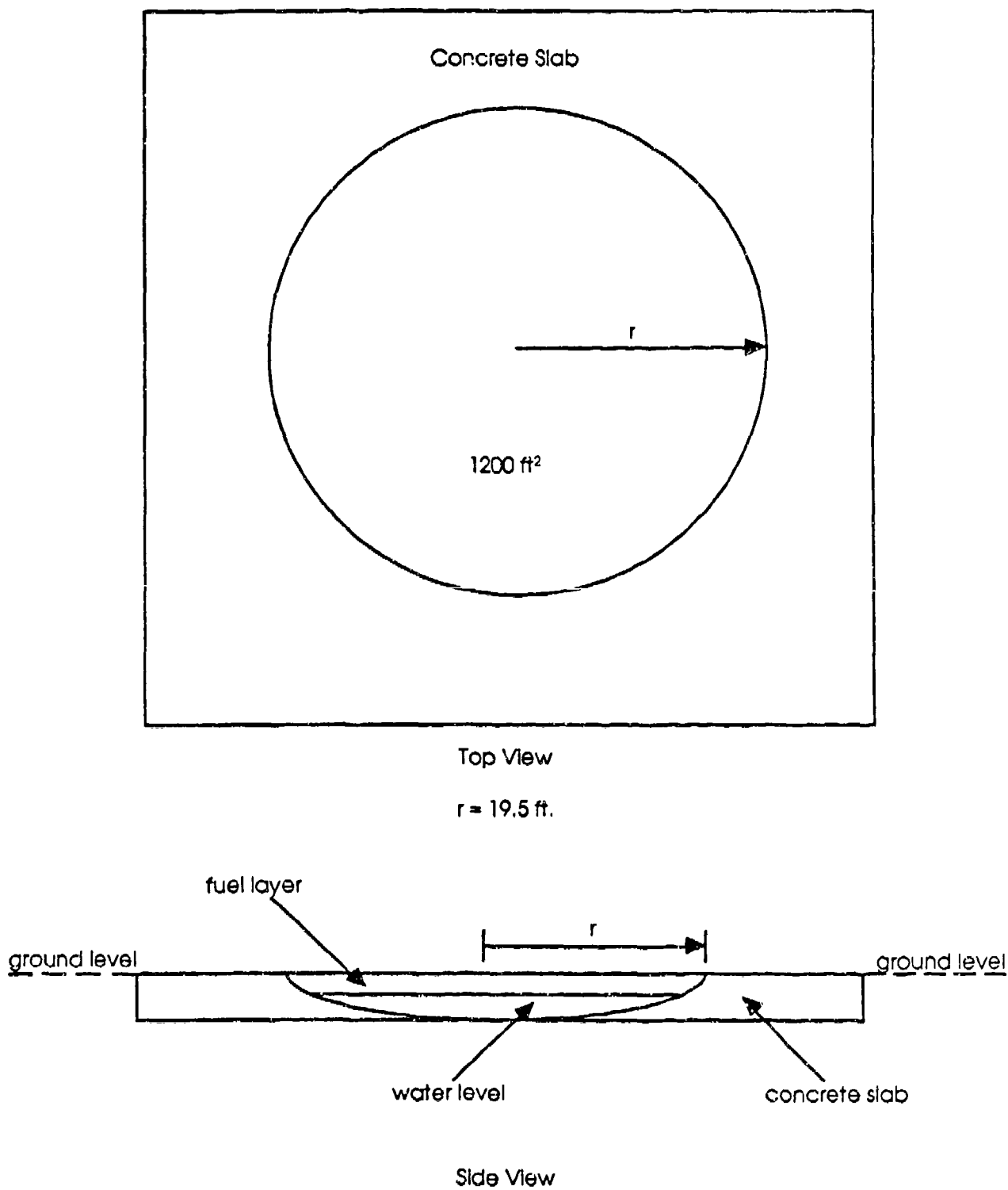


Figure 3. Fire Pit Configuration  
23

The following paragraphs detail the test configuration for each task.

#### 1. Task 1, 2, and 7 Test Configuration

The common factor between tests of Task 1, 2, and 7 is that the pool fires did not contain any simulated aircraft parts as did Tasks 3, 4, 5, and 6. The pool areas of Task 1 and Task 7 were held constant at 100 ft<sup>2</sup> and 4418 ft<sup>2</sup>, respectively. The pool area of Task 2 was either 300 ft<sup>2</sup> or 600 ft<sup>2</sup>. Figure 4 illustrates the general test configuration of these three tasks.

#### 2. Task 3 Test Configuration

As detailed in Section II, a thin metal ring was placed in the center of the pool before fuel application. This ring prevented fuel from entering the center of the pool. The result of this configuration was a pool fire in the annulus formed by the two rings and a nonflammable area at the pool center. Figure 5 details the general Task 3 test configuration. The inner areas were determined such that the minimum fire area is not less than 100 ft<sup>2</sup> and the ratio of inner to outer areas ranges from 5 percent to 50 percent.

#### 3. Task 4 Test Configuration

The Task 4 test configuration included an obstacle that could block suppression efforts to certain areas of the pool fire (See Section II). This obstacle consisted of a circular metal arc whose radius was smaller than the fire perimeter and tall enough to impede suppression efforts. The positions of the fire suppressors were fixed at 45 degrees on either side of the fire axis, parallel to the wind direction and upwind of the fire. Table 5 summarizes the pool areas and obstacle sizes that were used in Task 4. Figure 6 illustrates the general test configuration.

#### 4. Task 5 Test Configuration

The test configuration of Task 5 is similar to that of Task 4, except that, in addition to having an obstacle with suppression blocking abilities, as in Task 4, the obstacle will also have a high thermal mass. The test configuration illustrated in Figure 7 shows that the fire size is limited to 150 ft<sup>2</sup> and the object in the shape of a 4-foot radius half circle. The obstacle was constructed from aluminum or a mild steel. Two thicknesses were used for the steel slab, 1/4- and

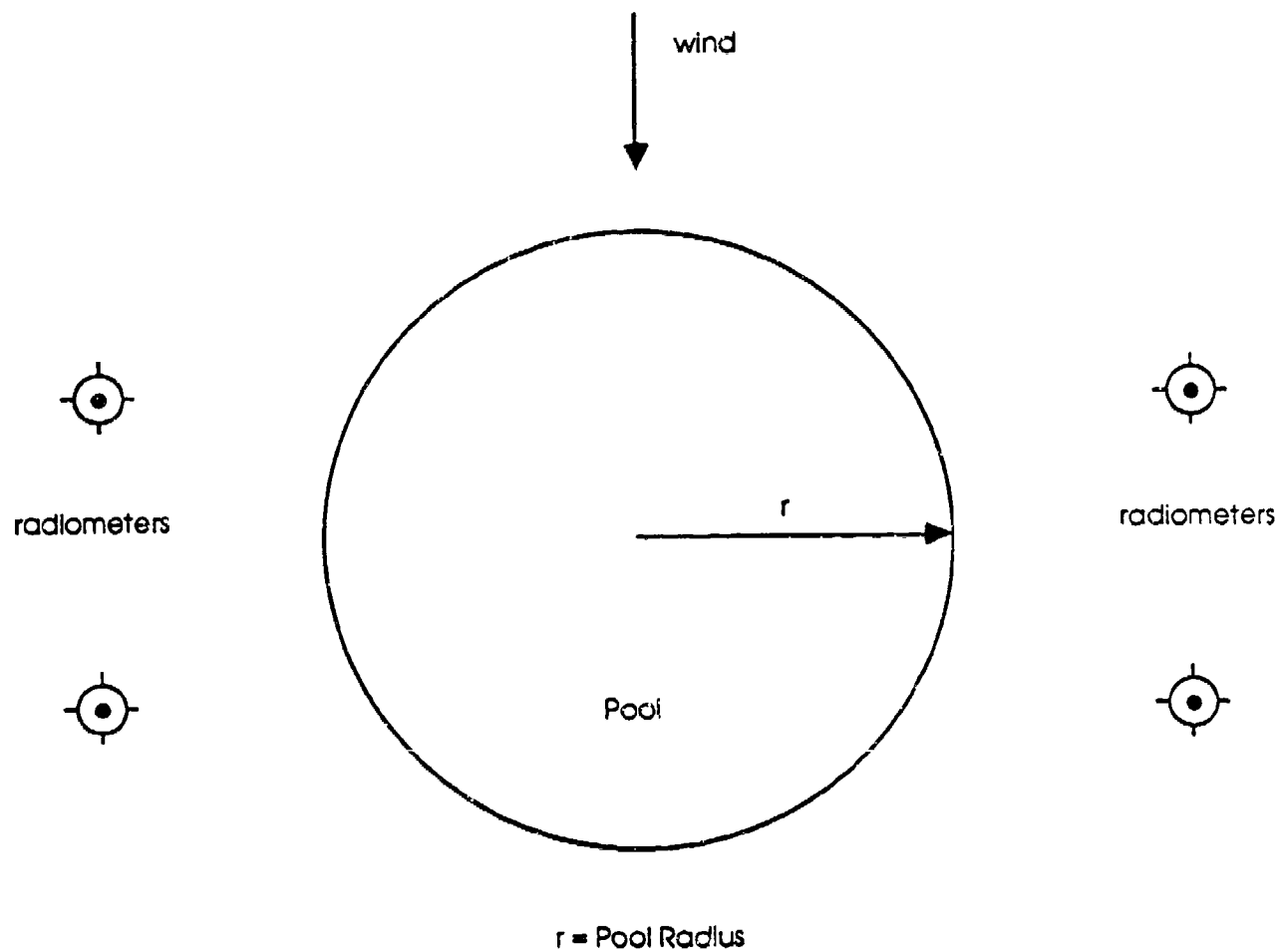


Figure 4. Task 1, 2, and 7 Test Configuration

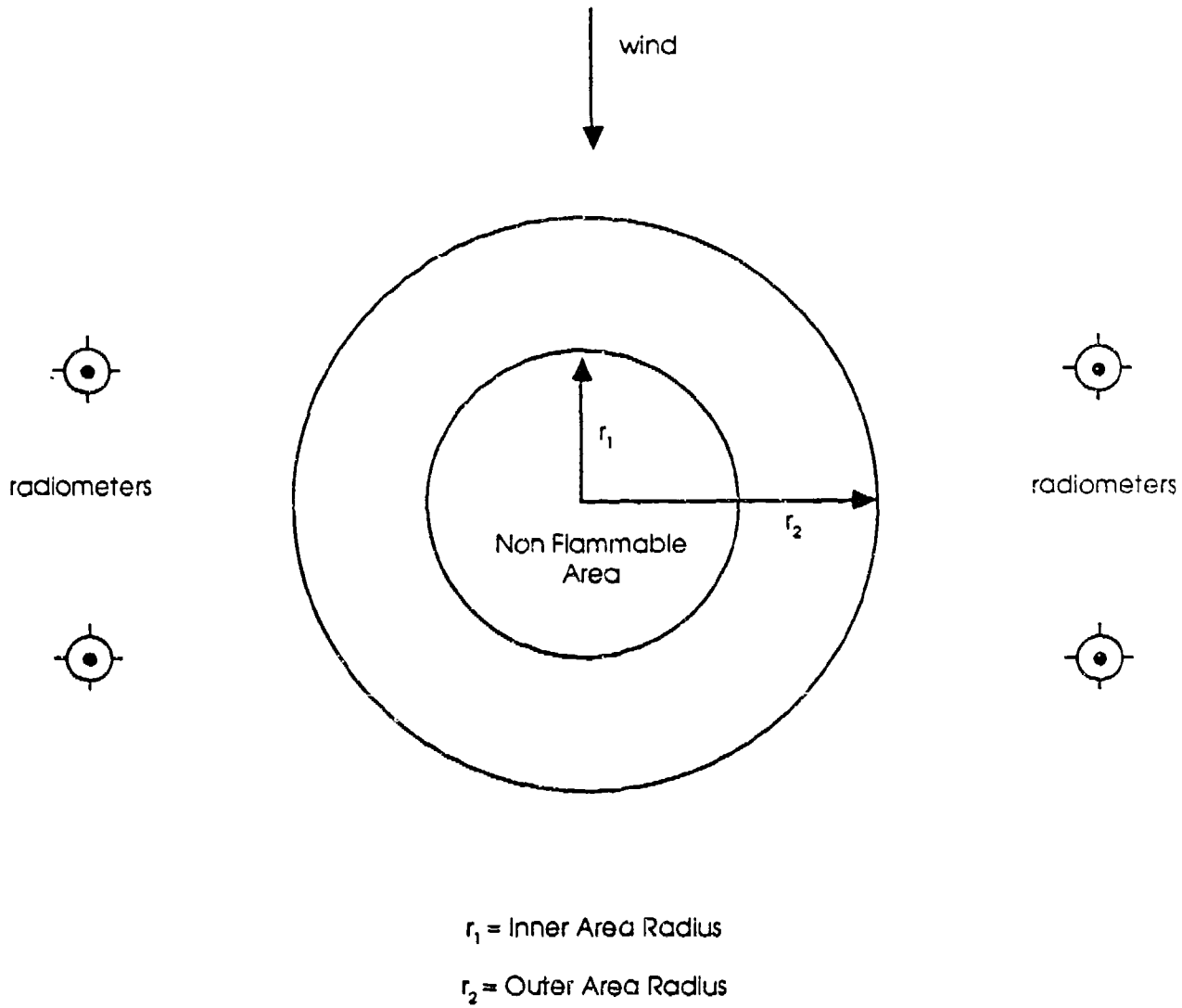


Figure 5. Task 3 Test Configuration

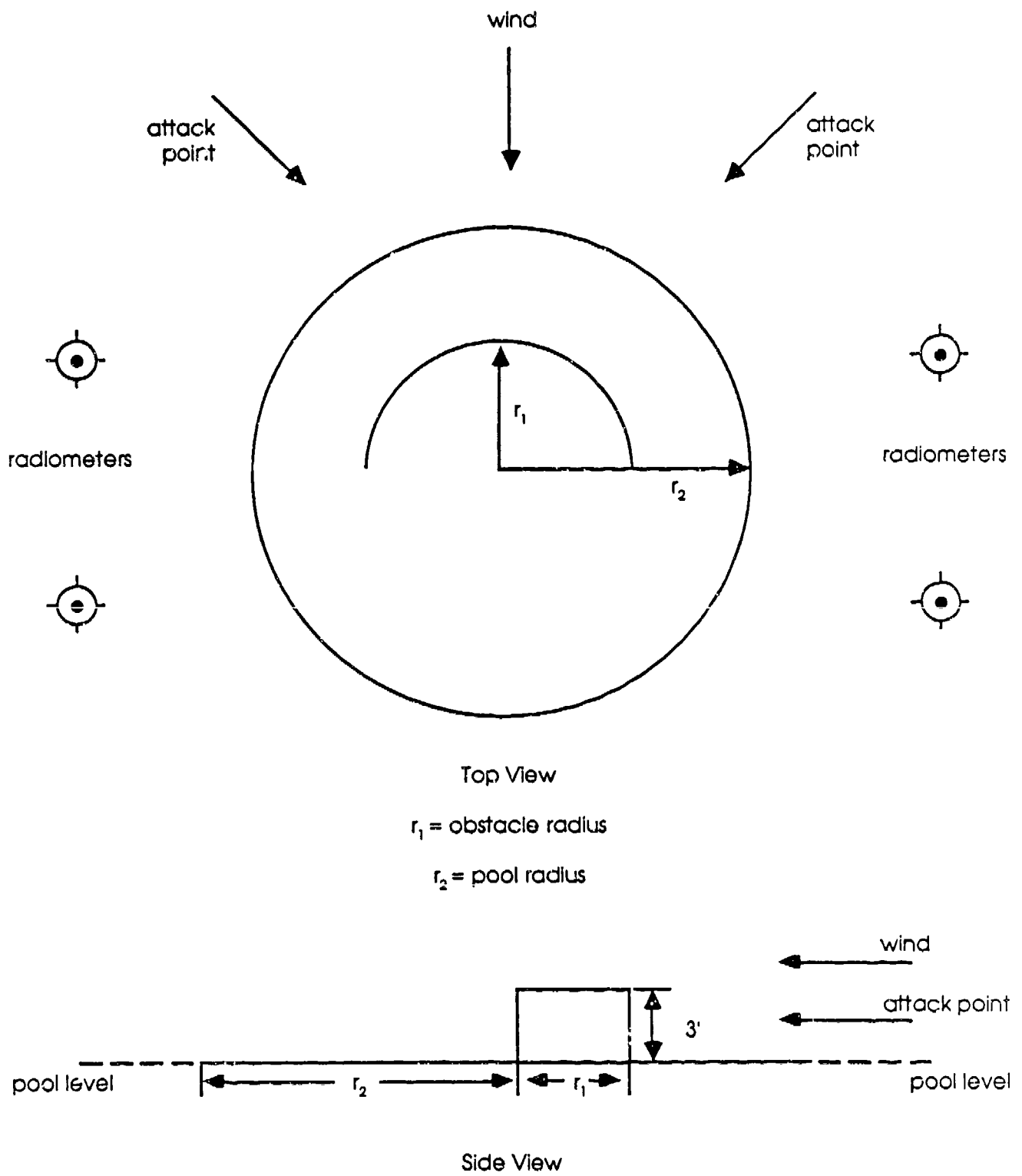
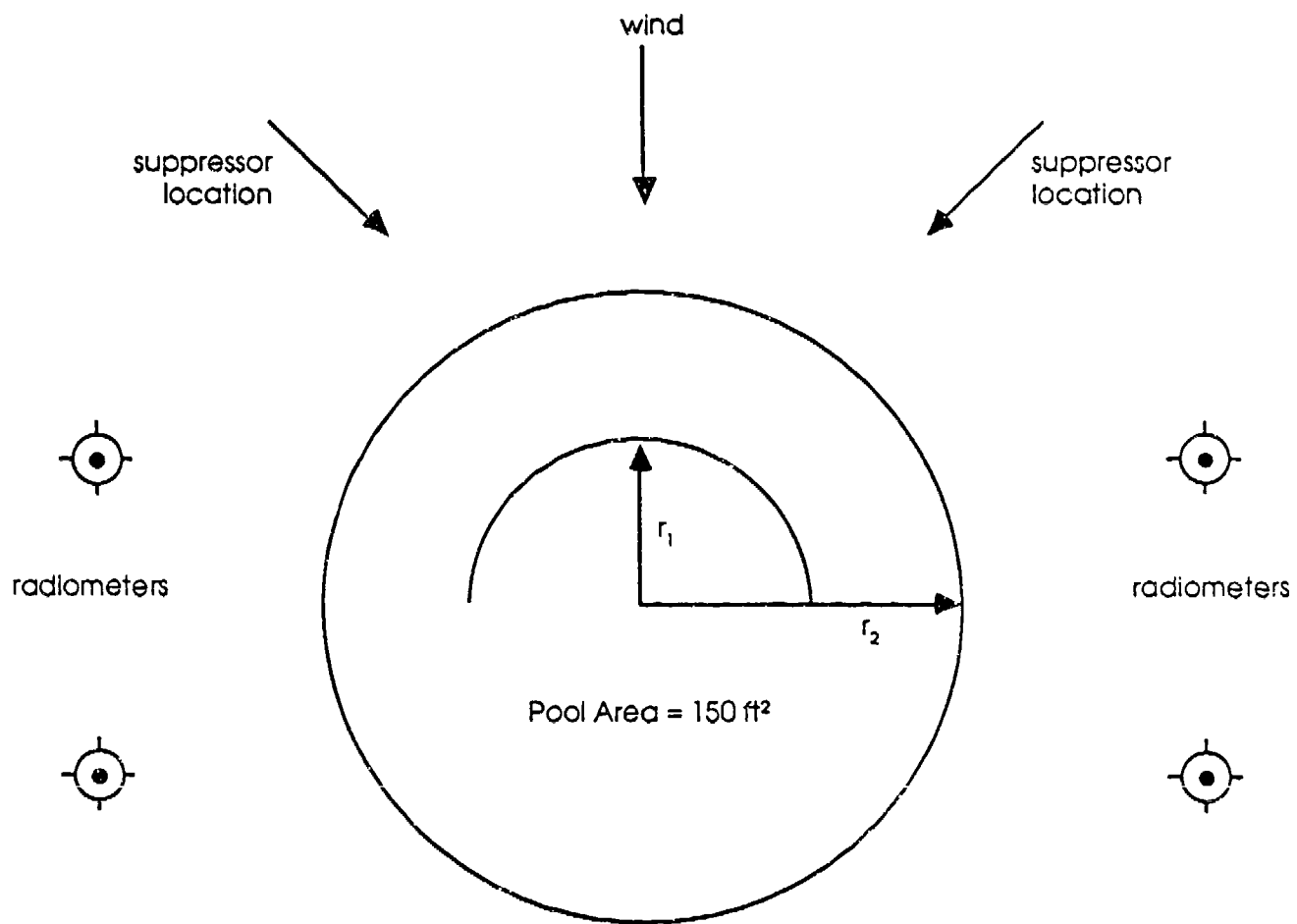


Figure 6. Task 4 Test Configuration



$r_1$  = obstacle radius = 3.99 ft.

$r_2$  = pool radius = 6.91 ft.

Figure 7. Task 5 Test Configuration

1/2-inch, while the aluminum slab used only a 1/4-inch thickness. The various obstacle parameters are summarized in Table 6.

As discussed in Section II, the obstacle temperature was monitored with thermocouples throughout each test. These thermocouples were grouped into two sets, with three thermocouples being in each set. The first set was placed near the top of the obstacle with a thermocouple being placed at the midpoint of each face and the third thermocouple placed in the interior of the obstacle. The second set was placed near the bottom of the obstacle, slightly above pool level, in a configuration identical to that of the first set. Figure 8 illustrates the thermocouple positions on the obstacle.

#### 5. Task 6 Test Configuration

The object of Task 6A testing was to study the effects on control time of a two-dimensional fire. This two-dimensional fire was achieved by allowing fuel to spread radially over a horizontal surface. This horizontal surface consisted of a packed, water-saturated clay. This effectively simulated a spill on smooth concrete, while avoiding the spalling, cracking, and other environmental problems associated with concrete. A continuous fuel source was located at the pool center at ground level. Following ignition, the pool continues to expand until the rate at which the fuel is consumed is equal to the input fuel rate, thus, making pool area a function of fuel flow rate and burn rate (See Section V). Control was attempted when the steady state-condition was achieved. The general Task 6A test configuration is illustrated in Figure 9. Table 7 outlines the various test parameters found in Task 6A testing.

#### 6. Task 6B Test Configuration

To determine the applicability of the model to three-dimensional pool fire configurations, an inclined plate was installed in the pit used for Task 6A. In Figure 10, the configuration of the test can be seen where the steel plate, 10 feet long and 3 feet wide, raised 5 feet at one end, was used as a simulation for an inclined aircraft wing. Fuel flowed from a continuous fuel source at the top of the ramp. There was no lip on the plate, allowing fuel to spill over the sides, as well as down the plate. As in the Task 6A configuration, the pool area depends on the fuel flow rate and the burn rate (See Section V). The various test parameters for Task 6B are outlined in Table 8.

Top View

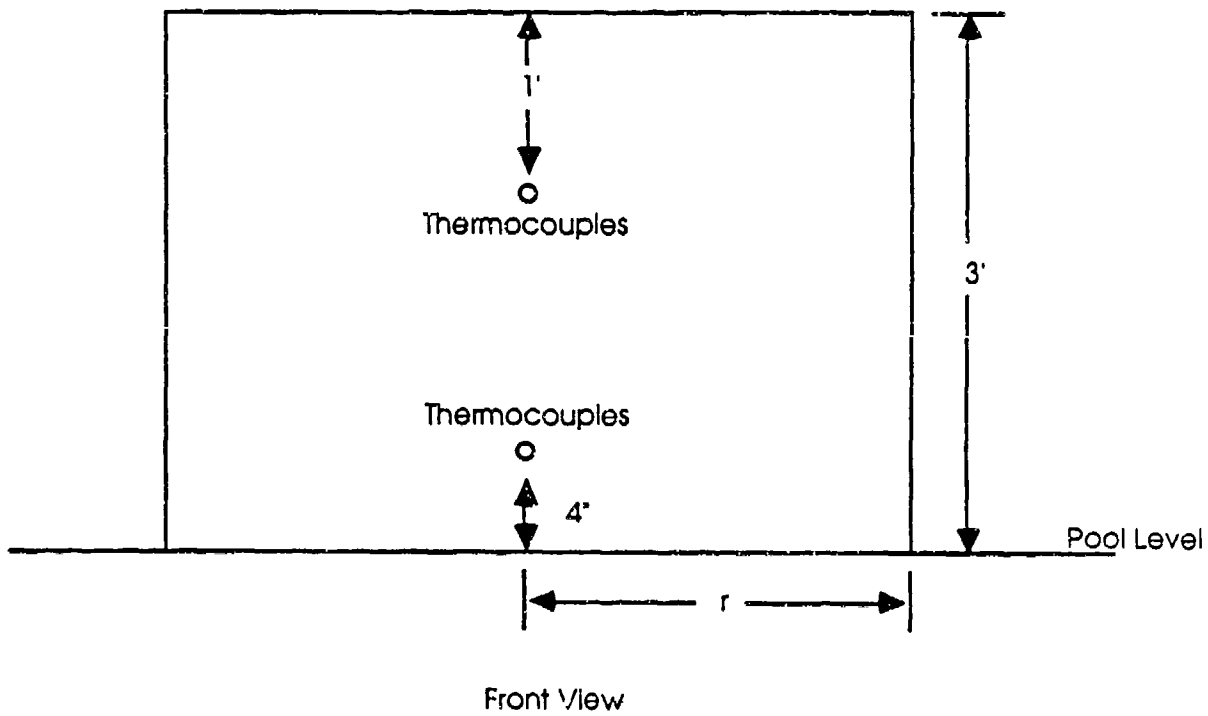
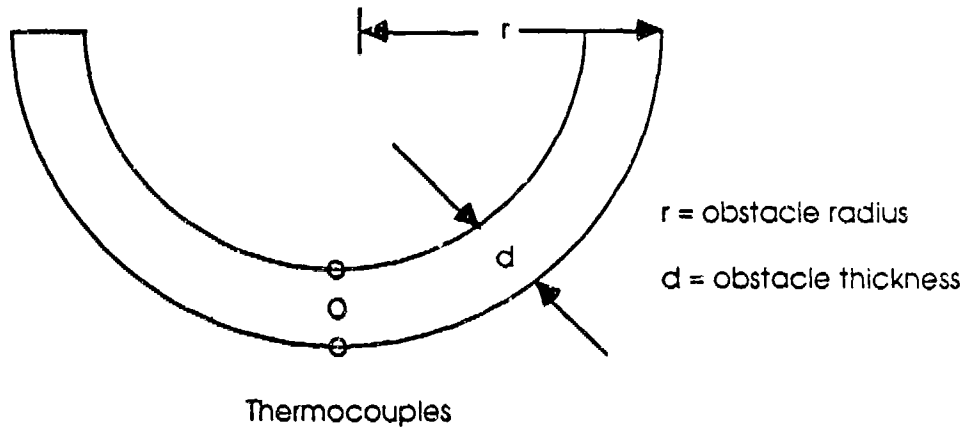


Figure 8. Task 5 Thermocouple Configuration

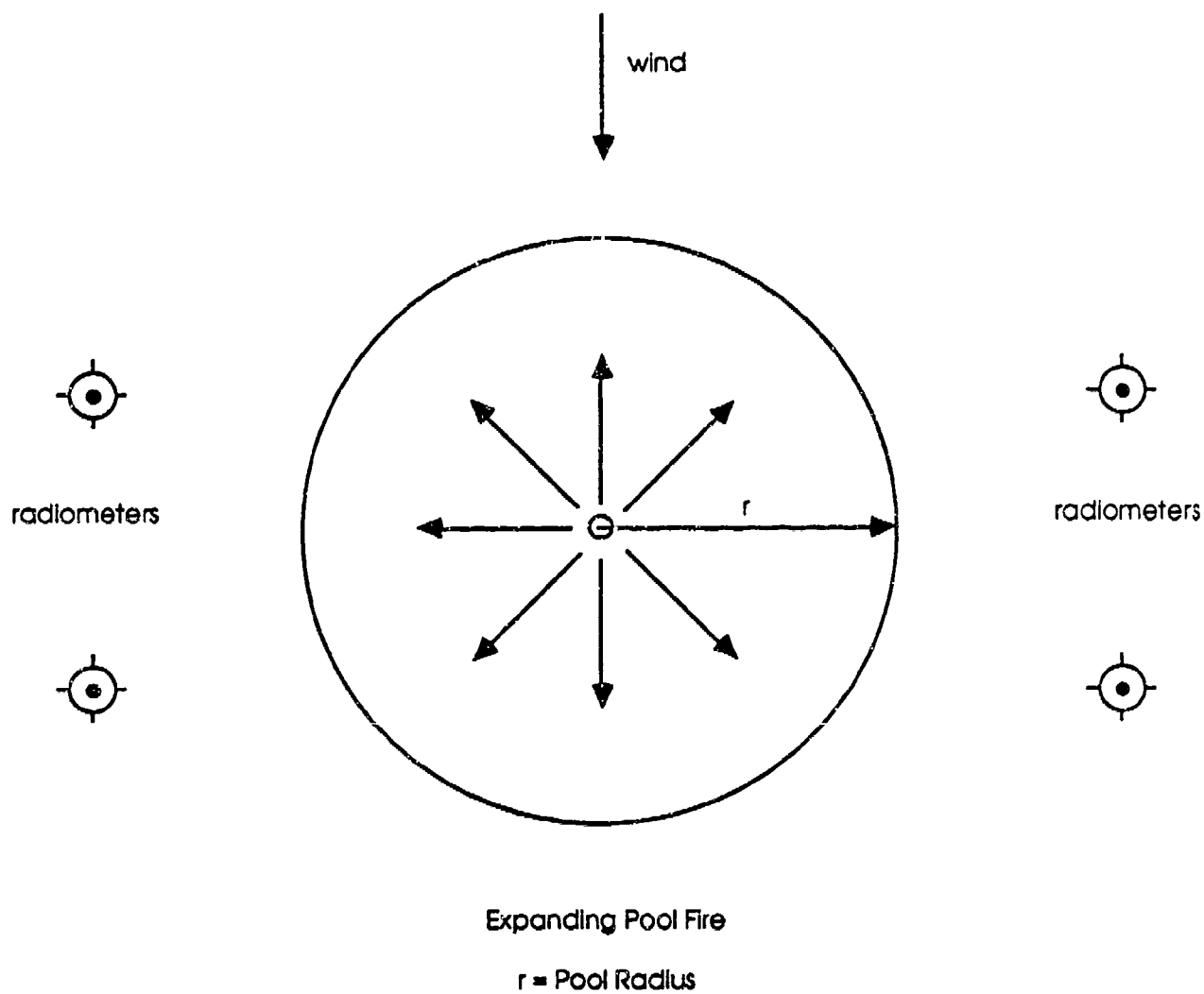
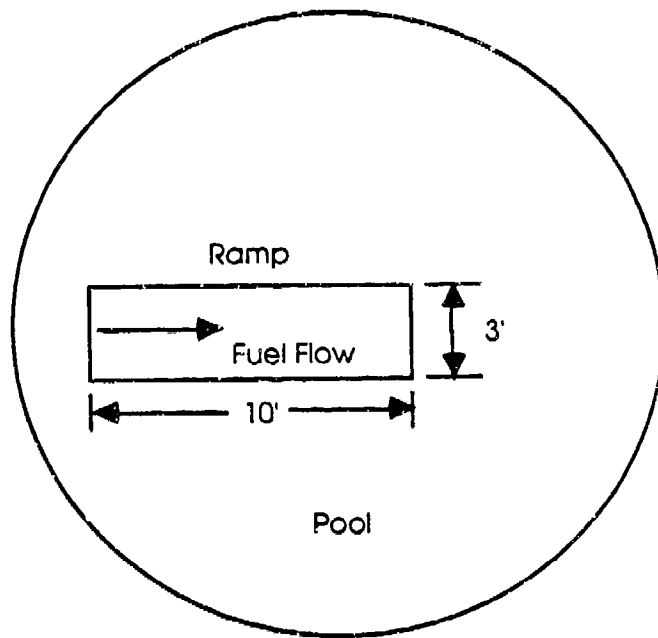
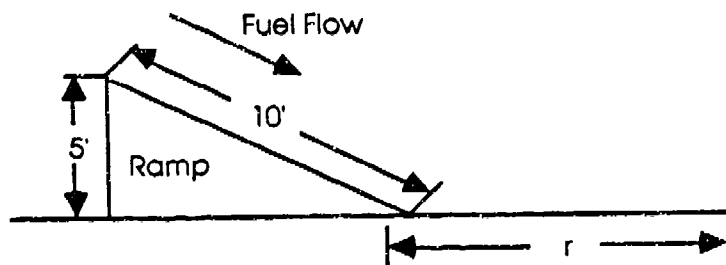


Figure 9. Task 6A Test Configuration



Top View



$r$  = Pool Radius

Side View

Figure 10. Task 6B Test Configuration

### C. TEST PROCEDURE

The following set of procedures was followed for each test burn.

1. The pool was either filled with a predetermined amount of JP-4 fuel (simple pool fire), or the fuel flow initiated (continuous source fires).
2. Recording was initiated for the appropriate instruments and the pool was ignited.
3. The fuel was burned for an empirically determined preburn time.
4. Fire suppression was started.
5. After the fire was extinguished, the pit was reignited to burn off the remaining fuel and foam.
6. The fire pit was prepared for the next test sequence.

### D. FIREFIGHTING PROCEDURE

All fires were ignited and suppressed by NMERI personnel trained in Air Force firefighting methods. The firefighters fought the fires as they would for an actual emergency fire. For each of the tests, they approached the tests from the upwind side. For two-person tests, each firefighter approached the fire at a 45 degree angle. In the tests where handlines were used, the handlines were connected to a premix solution tank in an Oshkosh model P-4 fire truck. The 4 different types of nozzles used on these handlines were the following:

1. Akron 1710 Turbojet
2. TFT Ultimatic 125
3. FEECON Cobra
4. Western Fire Forester

The nozzles were chosen for a fire based on the solution flow rate needed.

For the fires in Task 7 and one of the fires in Task 2, the turrets on the fire trucks were used to extinguish the fires. The Task 7 fires were fought with an Oshkosh P-19 fire truck using a FEECON bumper turret and an Akron spinning-tooth roof

turret. The first two fires of Task 7 were fought using the roof turret of the P-19. The third fire in Task 7 was fought with the P-19 using both the bumper and roof turrets for suppression. The fire in Task 2 was fought using the bumper turret on the P-4 fire truck.

Before every test, permission to burn was obtained from the control tower and the fire department. A safety officer was established to ensure that all safety rules concerning construction, the test site, and the fires were enforced.

## SECTION V

### THEORETICAL CONSIDERATIONS

This section reviews the derivation of the Phase 1 model and discusses the theory for the thermal mass tests of Task 5 and the derivation of a fuel-spread model for Task 6A.

#### A. PHASE I SUMMARY

The Phase 1 model was based on a theoretical expression for the spread of a high-viscosity fluid on a viscous (or solid) fluid surface. It was assumed that coverage of the fuel area by foam resulted in fire extinguishment. This model was originally developed to describe the spread of a high-viscosity liquid spilled instantaneously over a liquid with relatively lower viscosity. There were three spread regions:

1. The Inertia Region: Where gravitational and inertial forces dominate.
2. The Viscous Region: Where gravitational and viscous forces govern the spread of the liquid.
3. The Surface Tension Region: Where gravitational and surface tension forces dominate.

The radial spread in each region is given by the following relations:

#### Gravity-Inertia

$$r = 1.14 * (G * Q) * T \quad (1)$$

#### Gravity-Viscous

$$r = 0.98 * (G * Q / V) * T \quad (2)$$

#### Viscous-Surface Tension

$$r = 1.6 * (\rho / (\mu * \rho_w))^{1/2} * T^{3/4} \quad (3)$$

where

- T = control or extinguishment time
- G = effective gravity (ft/sec<sup>2</sup>)
- =  $g (1 - \rho_1/\rho_w)$
- g = gravitational acceleration (32.2 ft/sec<sup>2</sup>)
- $\rho_1$  = density of the spreading liquid (lb/ft<sup>3</sup>)
- $\rho_w$  = density of underlying liquid (lb/ft<sup>3</sup>)
- $\nu$  = kinematic viscosity of underlying fluid (ft<sup>2</sup>/sec)
- Q = total volume spilled (ft<sup>3</sup>)
- $\rho$  = surface tension (lb/sec)
- $\mu$  = viscosity of underlying fluid

By lumping all physical properties of the spreading and underlying liquids in Equations (1) - (3), substituting for Q the expression  $T^*AT$  where A = area and  $r = (A/\pi)^{1/2}$ , the following equation relating the total time,  $T_c$ , for foam spread (and thus, the control of the fire) to  $T^*$  and A can be derived

$$T_c = k_1 \frac{A^{1/3}}{T^{*1/3}} + k_2 \frac{A^{2/7}}{T^{*4/7}} + k_3 A^{2/3}$$

where  $k_1$ ,  $k_2$ , and  $k_3$  are constants.

The first term describes the initial spread of the liquid due to its inertial force overcoming gravitational forces. This term is not expected to be significant for the case of foam application from a turret or a nozzle. The last term describes the spread of liquid when a very thin molecular layer is left so that surface tension becomes important. This flow regime is probably not significant for the spread of foams on water. Therefore, foam spread may be modeled using only the second term of the last equation.

A statistical analysis on the equation  $t = k(A^{2/7}/F^{4/7})$  in Phase I determined that the coefficient k was 0.64 for non-obstacled fires and 0.518 for fires with obstacles present. The correlation coefficients, which are a measure of how well the data fits the model, were 0.774 and 0.760, respectively.

#### B. TASK 5 OBSTACLE HEAT TRANSFER MODEL

Section II shows that the objective of Task 5 is to determine how an object with a high thermal mass affects the control time of a pool fire. The large thermal mass object, placed in the center of the pool, was in the form of a circular metal arc that had a radius of 4 feet (Figure 7). The metal object, with large thermal conductivity, can quickly transfer energy from areas of high-temperature to low-temperature. The thickness of the plate, and the thermal conductivity determine how quickly the energy is transferred for a given temperature

differential. In the case of a metal plate in a fire, the steel plate absorbs a certain amount of thermal energy from the fire and, the temperature of the plate increases. Due to a large thermal conductivity, the center of the plate is also heated to a high temperature. During fire suppression, the surface of the plate is quickly cooled by a direct application of foam. After the fire is suppressed, the surface temperature of the plate will rapidly increase as energy is transferred to the surface from the center of the plate. The main concern of Task 5 was that this surface temperature exceed the autoignition temperature of the fuel to investigate whether reignition of the fuel would occur.

To estimate that the object obtained a temperature above the autoignition temperature of JP-4, a computer model was developed to determine the amount of time needed for the center of an object of a given thickness to reach a specified temperature. The basis of this model was a one-dimensional heat transfer equation with appropriate boundary equations. The coupled equations were then solved numerically. The equation is represented by

$$q = k * A \, dT / dx$$

where       $q$  = Heat Flux  
              $k$  = conduction Coefficient  
              $A$  = Unit Area  
              $dT$  = Delta Temperature  
              $dx$  = Delta Thickness

Due to the symmetry of the problem, the model specified an insulated flat plate of half the desired thickness, with negligible edge effects. The initial temperature of the plate was assumed to be 70 degrees Fahrenheit while the total heat flux at the surface was assumed to be 30,000 Btu /ft<sup>2</sup>-hr. Various numerical simulations were performed, using the computer program developed specifically for this problem. A major uncertainty associated with the application of the model, is the cooling associated with direct application of the foam on the metal surface. To account for this uncertainty in applying the computer results to the experimental design, a multiplicative factor was applied to the estimated heating time to help achieve surface temperatures after cooling and reheating above the autoignition temperature.

Figure 11 is a result of one simulation, in which it was assumed that the average flame temperature at the surface of the heated object was 1500 degrees Fahrenheit. This figure shows the time needed to heat the center temperature of the object to 1500 degrees Fahrenheit, based on the thickness of the object.

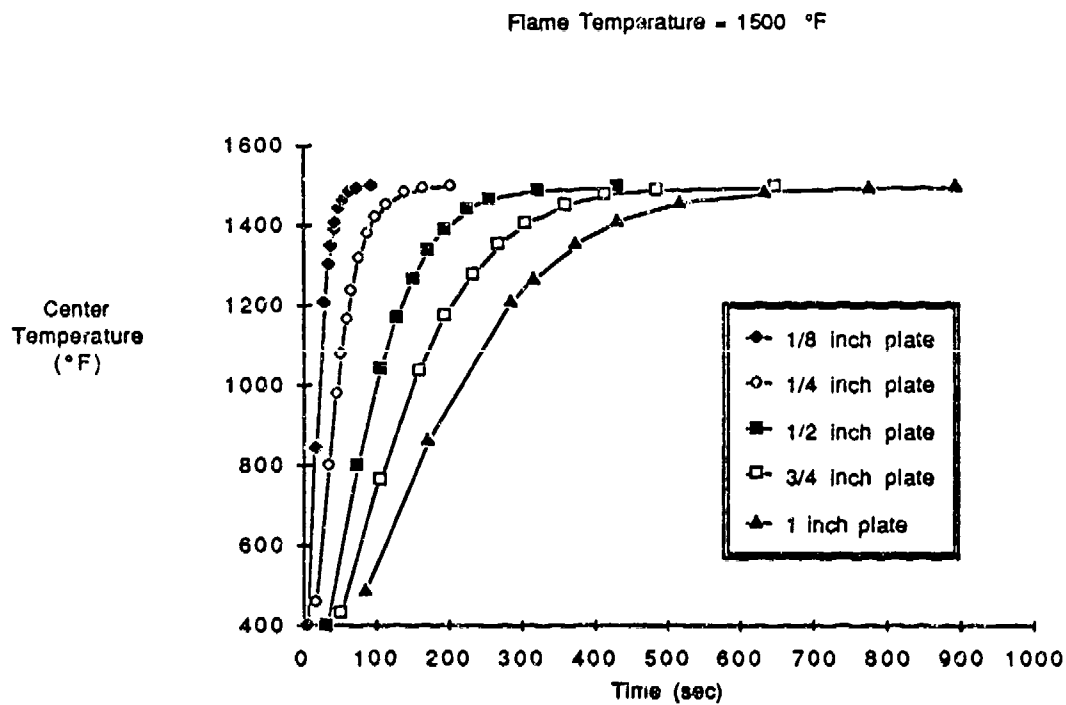


Figure 11. Thermal Mass Heat Transfer Simulation

### C. TASK 6 EXPANDING POOL MODEL

In Task 6 the applicability of the theoretical suppression model to two and three dimensional fires was studied (See Section II). In Task 6A, a two-dimensional pool fire is defined as a burning pool that has a continuous fuel source and is expanding radially. In Task 6B a three-dimensional pool fire is defined as burning fuel that first moves down a ramp then forms an expanding burning pool at the base of the ramp (See Section IV). In Task 6A and 6B, these expanding pools will reach an equilibrium where the fuel consumed is equal to the fuel flow rate. When this equilibrium is reached, the pool will stop expanding. It was necessary to know this equilibrium pool area for a given fuel flow rate before actual testing began to choose an appropriate size fire pit and find a way to express the fire area used to predict control time. This was accomplished by developing a computer model for a simple gravity-spread fluids model, as well as a simple mass conservation determination between the fuel flow rate and the burn rate. The results of this prediction model can be seen in Figure 12 where it can be seen that a 30 foot diameter pit was sufficient for our purposes.

The gravity spread model assumed that flow is in the radial direction, and is summarized by

$$Q = \rho \cdot V \cdot dA \cdot dt - M_b \cdot dA \cdot dT$$

where

- Q = Mass Flow of Fuel
- dA = Delta Area = dR \* dH
- dR = Delta Radius
- dH = Delta Liquid Height
- dt = Delta Time
- V = ( 2 \* g \* dH )<sup>1/2</sup>
- rho = density of fuel
- g = gravitational constant
- Mb = Mass Burn Rate / Unit Area.

The mass balance model assumed that

$$M_b = M_f$$

where

- Mf = Mass Flow of the Fluid onto a surface.

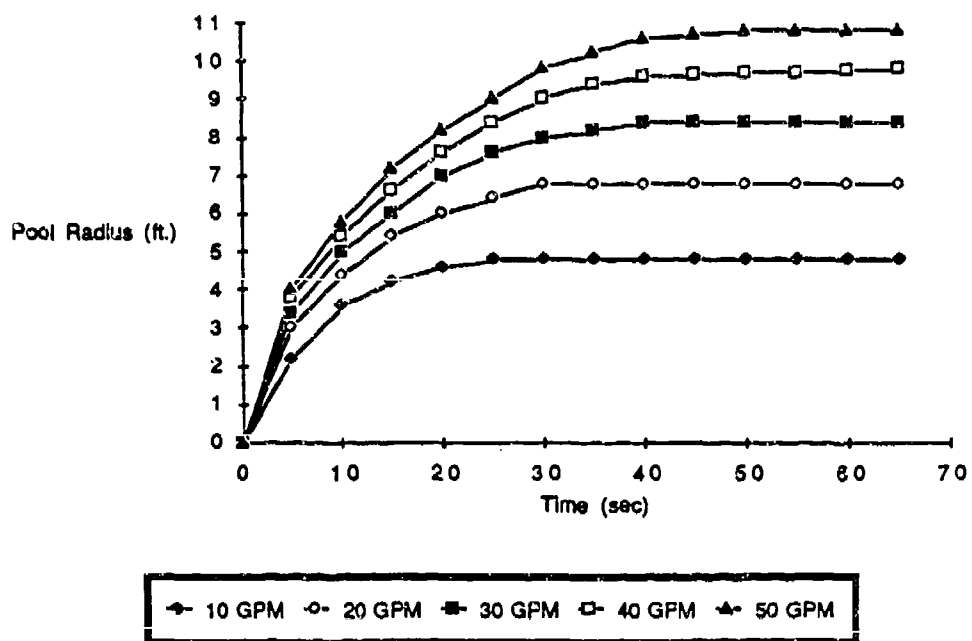


Figure 12. Pool Radius vs Time for Expanding Pool Fire

## SECTION VI

### DATA ANALYSIS

This section reviews the manner in which control times were determined from the radiometer data and the statistical methods that were used in model development.

#### A. DETERMINATION OF CONTROL TIME FROM RADIOMETER DATA

Control times were obtained from the radiometer readings. The criterion for control time was the time at which the heat flux, as measured by the radiometers, reached 10 percent of the maximum steady-state value. Techniques were needed to determine the time at which the heat flux reached 10 percent of the maximum value and average the data so that one representative control time would be determined from the four individual radiometers.

##### 1. Determination of 10 Percent Value of Heat Flux

Control time, for this series of experiments, was defined to be the time at which the radiant flux of the fire reached 10 percent of the maximum steady-state value, as measured by the radiometers. Because of the transient nature of the fires, this was not a straight-forward task. Figure 2 presents a time history of the heat flux of a fire. Many random spikes resulting from the flickering flame. This complicates the task of establishing a steady-state maximum heat flux and determining the time at which the flux is 10 percent of that value.

The maximum steady-state heat flux was determined by averaging all the points 5 seconds before suppression began. This seemed to be appropriate since the fluxes had already settled to a steady state. Averaging the data eliminated the spikes that occurred. To select the 10 percent value, a more sophisticated method was used. A curve was regressed between the point at which suppression was initiated and the time at which the heat flux reached a level below 10 percent of the maximum heat flux. The curve was regressed as a fifth-order equation with time as the dependent variable and radiometer flux as the independent variable. The control time was then calculated by using the equation of the newly regressed curve and the 10 percent value. This method essentially averaged the curve between suppression initiation and the 10 percent value while providing an analytical means of calculating the control time from the 10 percent value.

## 2. Control Time Selection

Once a control time has been determined for each radiometer, a procedure was needed to eliminate faulty radiometer readings and to obtain one representative control time from the remaining control times.

Great care was taken so that each radiometer would be spaced apart so that flux readings would be representative of their location and independent of the other radiometer readings. This was done to obtain an unbiased view of the fire. However, occasionally a radiometer's field of view may have been blocked by a stream of foam, or the steam resulting from the foam being sprayed on the fire. This would result in an artificially low flux reading. If a radiometer had been in the flame this would have resulted in a flux reading that was unreasonably high. To eliminate faulty radiometer readings, a 95-percent confidence interval was calculated to accept or reject each radiometer control time. A confidence interval is a statistical method of determining whether a data point belongs to a related data set. A 95 percent confidence interval suggests that there is a 95 percent probability that the data contained within the interval belongs to a related data set. For a small sample, the 95 percent confidence interval is bounded by the values

$$\bar{x} - t_{0.975} S/(N - 1)^{1/2} \quad \text{and} \quad \bar{x} + t_{0.975} S/(N - 1)^{1/2}$$

where  $\bar{x}$  = the mean of the sample  
 $t_{0.975}$  = The 97.5 percentile of the t statistic with  
 $N - 1$  degrees of freedom.  
 $N$  = the size of the sample  
 $S$  =  $((1/N)(\sum x_i^2 - N\bar{x}^2))^{1/2}$

Once the interval was constructed, each control time of a test was tested to determine whether it was within the interval. The control times not within the interval were rejected and all values within the interval were averaged to form one control time for a particular test.

## B. STATISTICAL ANALYSIS

The method of analysis used on the Phase II data sets consisted of fitting data sets to the Phase I model using a multiple linear regression technique. A sweep algorithm was used to compute the least squares estimates  $B(i)$  and the associated regression statistics for the equation

$$\hat{y}_k = B_0 + \sum_{i=1}^{n-1} B_i x_{ik}$$

The analysis minimizes the residuals of the control time  $e_k$

$$e_k = y_k - \hat{y}_k$$

where  $y$  is the observed value of the depend c variable for case  $k$  and  $\hat{y}$  is the predicted value.

The statistics of primary interest are the sample correlation coefficient (most often shown as the square of the correlation coefficient) and the standard error of estimate. The correlation coefficient is given as:

$$r = \frac{n \sum xy - \sum x \sum y}{\left\{ \left[ n \sum x^2 - (\sum x)^2 \right] \left[ n \sum y^2 - (\sum y)^2 \right] \right\}^{1/2}}$$

The coefficient always lies between -1 and +1. If, and only if, all points lie on the regression line, then  $r = +1$ . If  $r = 0$ , the regression does not explain anything about the variation of  $y$ , and the regression line is horizontal. If the  $r$  squared value is found to be 0.80, then the regression of  $y$  on the independent variable accounts for 80 percent of the variance of  $y$ .

The scatter in the vertical ( $y$ ) direction of the observed points about the regression plane is measured by the standard error of estimate (SE):

$$SE = \left\{ \frac{1}{(n-k-1)} \sum_{i=1}^n (y_i - \hat{y}_i)^2 \right\}^{1/2}$$

If the standard error is based on a sufficiently large sample, it is a good estimation of the scatter of the population about the true or population regression plane. If the deviations from the plane are normally distributed, about 95 percent of the points in a large sample will lie within  $\pm 2$  SE of the plane (measured in the y direction). If the deviations are approximately normally distributed, about 68 percent of the observed values should lie within the SE of the plane.

## SECTION VII

### DATA PRESENTATION

In this section the data for all tasks is presented in raw form and the relation between control time and foam application rate for different pool areas is investigated. The relation between burn rate and pool area is also explored. In addition, three different factors and their effects on control time are investigated; the effects of windspeed, the effects of the expansion ratio of the foam, and the effects of one-person vs two-person attacks.

#### A. EFFECT OF POOL AREA ON BURN RATE

Figure 13 is a plot of burn rate in lbs/sec vs pool area for three different pool areas. The relation is linear implying that the burn rate in units of lbs/ft<sup>2</sup>-sec is constant. The burn rate is approximately equal to 0.0175 lbs/ft<sup>2</sup>-sec.

#### B. CONTROL TIME VERSUS APPLICATION RATE

Figures 14 - 20 are plots of control time vs application rate for each task. For Task 6B fires, the criterion for control was redefined as the time it takes for the heat flux to reach 25 percent of the maximum steady-state flux instead of the 10 percent value used for all other tests. This was done because no Task 6B fires were controlled using the 10 percent control time criteria.

The plots of the tasks all exhibit the same pattern of exponential decay. There are two threshold application rates present in each task beyond which foam application rates do not influence control times. There is a minimum application rate below which it takes a disproportionately long time to control certain fires and there is a maximum application rate above which there is not a decrease in the control time due to additional foam application.

In Figure 14, representing Task 1 fires, there is a noticeable trend upwards in control times for foam application rates below 0.025 gal/ft<sup>2</sup>-min for the Task 1 fires. This suggests that for application rates below 0.025 gal/ft<sup>2</sup>-min control of the Task 1 fires takes a longer time or is not

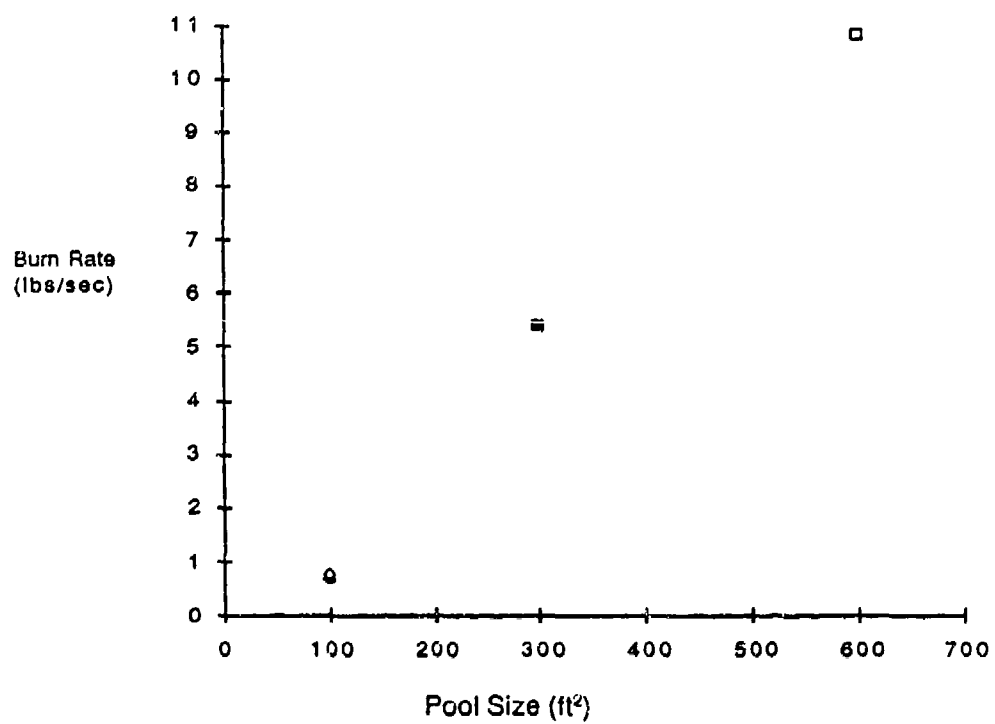


Figure 13. Burn Rate vs Pool Area

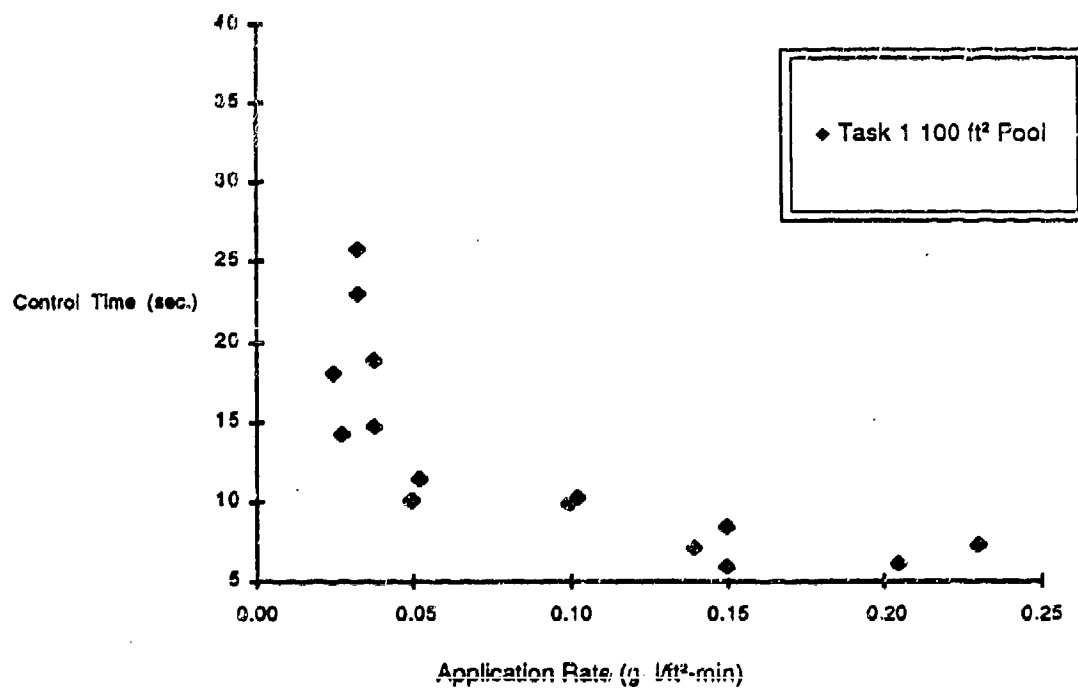


Figure 14. Task 1 Data

possible. This minimum application rate appears to increase with the complexity of the fire. In Figure 16 representing the Task 3 annulus fires, the minimum application rate appears to be at 0.05 gal/ft<sup>2</sup>-min. In Figure 17 representing the Task 4 and 5 barrier fires, the minimum application rate is approximately 0.06 gal/ft<sup>2</sup>-min. In Figure 18 the minimum application rate for the Task 6A two-dimensional fires is 0.10 gal/ft<sup>2</sup>-min. It is also for certain application rates below 0.10 gal/ft<sup>2</sup>-min, control of the fire was not possible in Task 6A.

Conversely, there appears to be a maximum application rate beyond which the control time remains constant. This implies that for any application rate beyond this maximum, the additional foam is wasted since it does not decrease control time. The most obvious examples of this are in Figures 15, 17, 18, and 19. This maximum application rate does not appear to change with the complexity of the fires. It appears to be at approximately 0.15 gal/ft<sup>2</sup>-min for all the tasks.

There is, thus, a bounded interval for which there exists a relation between foam application rate and control time. Application rates below the minimum bound result in control times unpredictably high, while application rates above the maximum bound do not decrease control times.

Figure 20 is a plot of control times vs application rate for various areas for the simple pool fires of Tasks 1, 2, 3, and 7. There does not seem to be an effect of area on control time for these tasks.

#### C. EFFECT OF WINDSPEED ON CONTROL TIME

Most of the testing took place at relatively low windspeeds (less than 15 mi/hr). For the few tests that occurred at windspeeds above 15 mi/hr, there were noticeable difficulties in applying the foam. The wind would bend the foam stream and carry the foam further in the air. Thus, some of the foam intended for a specific target would be sprayed elsewhere due to the wind. There were no noticeable wind effects for wind speeds less than 15 mi/hr. Figure 21 is a graph of normalized control time vs windspeed. There does not seem to be a corresponding increase in control time as windspeed increases. Therefore, for windspeeds less than 15 mi/hr there are no effects of wind on control times.

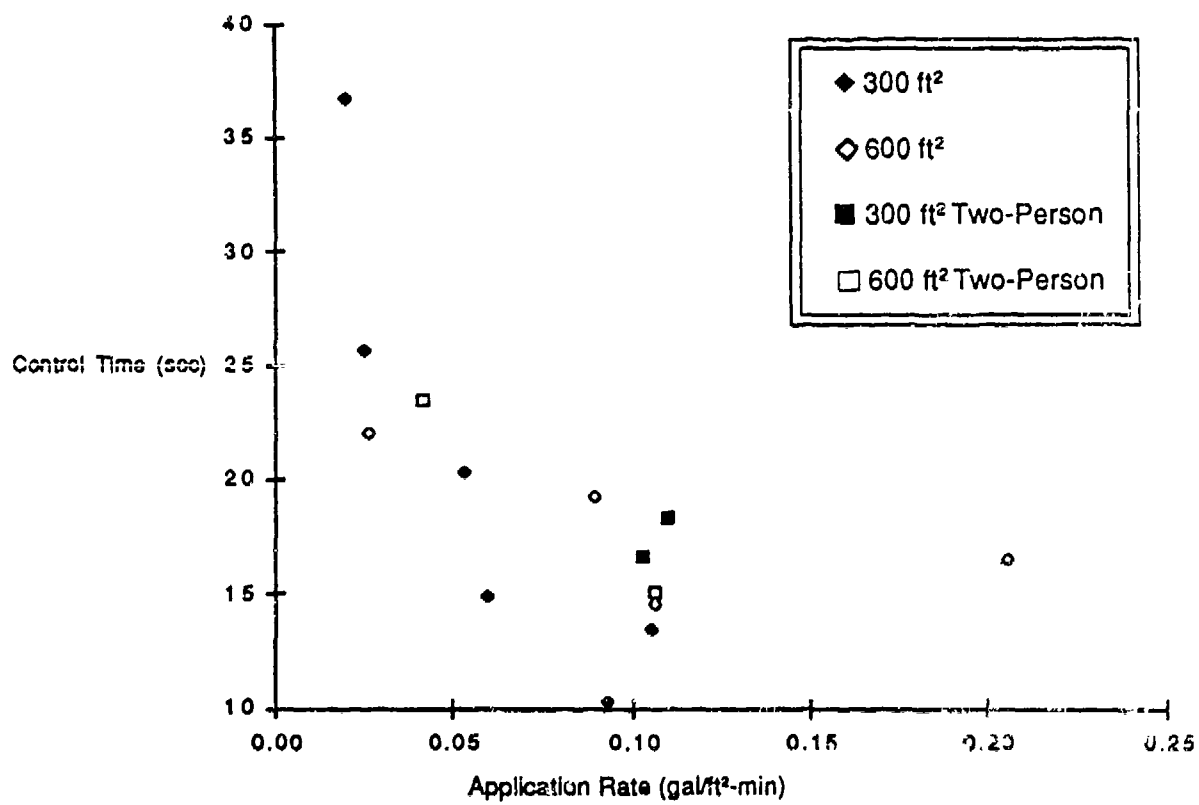


Figure 15. Task 2 Data

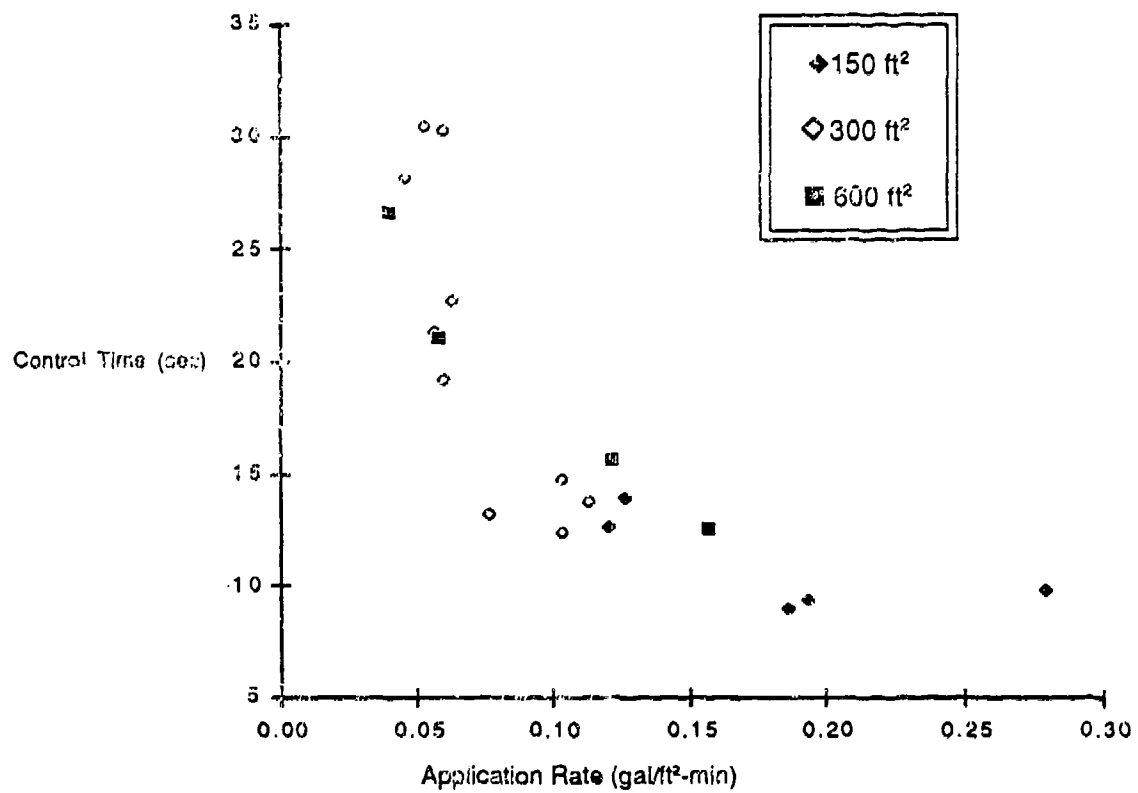


Figure 16. Task 3 Data

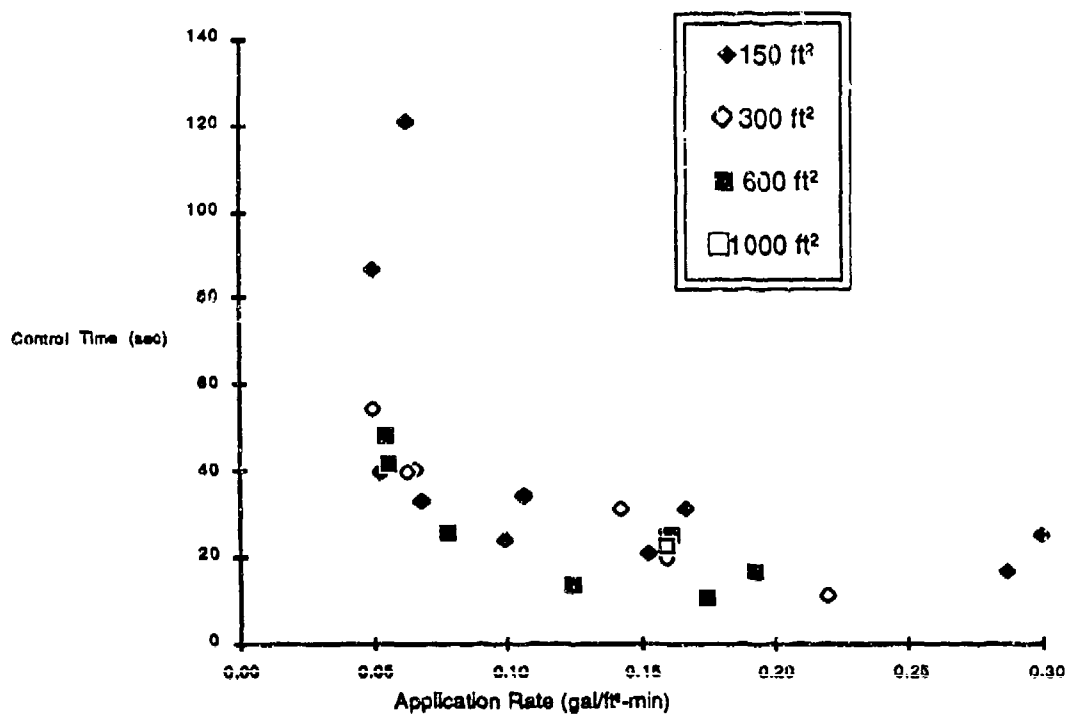


Figure 17. Tasks 4 and 5 Data

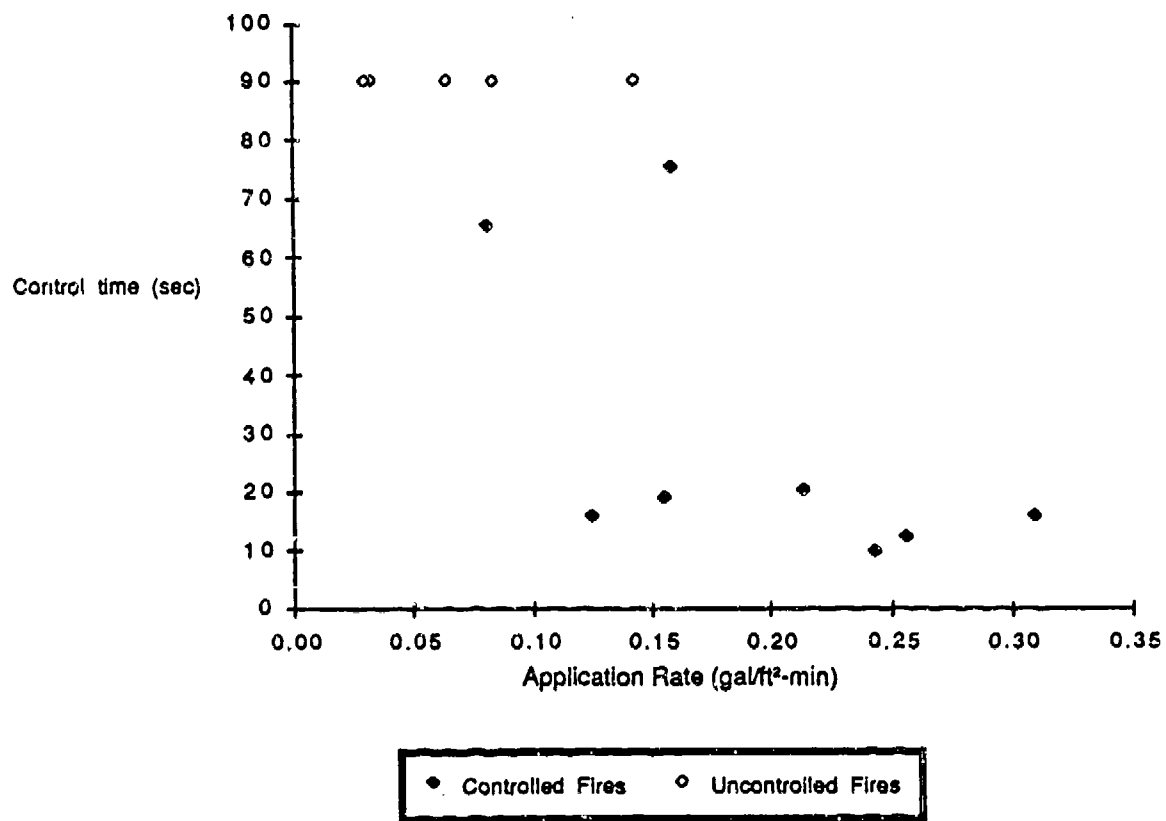


Figure 18. Task 6A Data

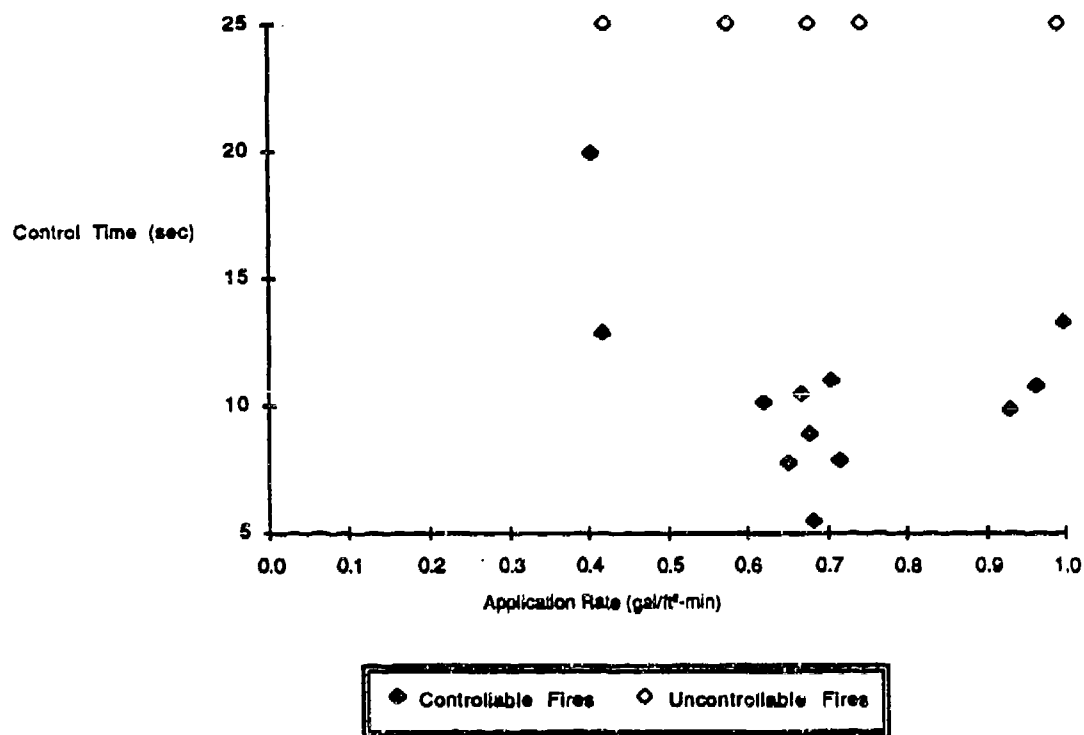
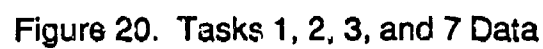


Figure 19. Task 6B Data



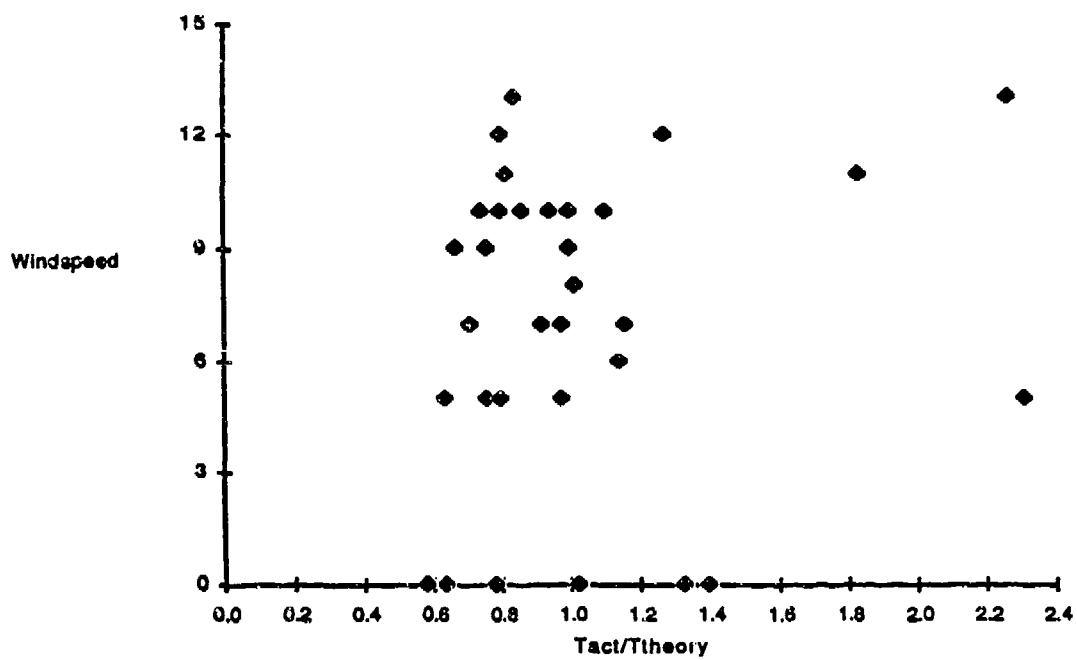


Figure 21. Effects of Wind Speed on Control Time

#### D. EFFECT OF FOAM EXPANSION RATIO ON CONTROL TIME

AFFF expansion ratios were measured to determine whether they had an effect on control time. Figure 22 is a plot of normalized foam expansion ratio vs control time for the various nozzles used in Tasks 1, 2, and 7. The foam expansion ratios were normalized by dividing them by the foam flow rates that were used for each test and were expressed in units of milliliters/gram-gpm (ml/gram-gpm). This was done to resolve the effects of the foam expansion from the effects of foam application rate. As shown in Figure 22, there is no clear relation between the foam expansion ratio and control time. It can be concluded that for this set of experiments, foam expansion ratio did not have an effect on control time.

#### E. EFFECT OF TWO-POINT ATTACKS ON CONTROL TIMES

In Task 2, the effect of two-person attacks vs one-person attacks was investigated. Pool areas and application rates were held constant and for these tests. Figure 15 is a plot of control time vs application rate for one- and two-person attacks. The diamonds and X 's represent two-person attacks for 300- and 600-ft<sup>2</sup> fires while the squares and triangles represent one-person attacks for the 300- and 600-ft<sup>2</sup> fires. There does not seem to be a difference in control time resulting from the addition of the extra firefighter.



## SECTION VIII

### MODEL RESULTS

Data from all tasks was regressed against the Phase 1 model. For the more complex fires of Tasks 3, 4, 5, and 6A, additional terms were developed to account for the variations in the foam flow necessary to cover the area of a particular fire configuration. The basic assumption maintained in the development of these models is that the control time is directly related to the time it takes for the foam to completely cover the fire pool area. The end result was the development of one comprehensive model capable of predicting control times for all the different fire configurations studied in this program except three-dimensional fires. Table 10 summarizes the different models that were developed and the results that were obtained.

#### A. TASK 1 RESULTS

Task 1 consisted of 100 ft<sup>2</sup> pool fires with foam application rate as the only variable. The Task 1 test data were regressed against the Phase 1 model equation:

$$T = C * A^{2/7} / F^{4/7}$$

The empirical coefficient was equal to  $C=0.6777$ . The Sample Correlation Coefficient had a value of  $r^2 = 0.946$ , denoting a strong relationship between the theoretical model and the physical data. The Standard Error of Estimate was 3.39 seconds.

#### B. TASK 2 RESULTS

Task 2 consisted of pool fires of different pool areas but with the same foam application rates as Task 1. The data were regressed against the Phase 1 model

$$T = C * A^{2/7} / F^{4/7}$$

and the value of the empirical coefficient was  $C=0.6458$ . The Sample Correlation Coefficient was found to be  $r^2 = 0.954$  and the Standard Error of Estimate was 4.60 seconds.

TABLE 10. SUMMARY OF MODEL EQUATIONS AND THEIR REGRESSION RESULTS

Task #	Model Equation	C	r <sup>2</sup>	Standard Error
1	$T = C * A^{2/7} / B^{4/7}$	0.6777	0.946	3.39 sec
2	$T = C * A^{2/7} / B^{4/7}$	0.6458	0.954	4.60 sec
3	$T = C * A^{2/7} / B^{4/7}$	0.8239	0.958	4.02 sec
4	$T = C * A^{2/7} / B^{4/7}$	1.4049	0.920	8.72 sec
5	$T = C * A^{2/7} / B^{4/7}$	1.8652	0.979	4.69 sec
6A	$T = C * A^{2/7} / B^{4/7}$	1.6570	0.934	4.48 sec
6B	$T = C * A^{2/7} / B^{4/7}$	2.8080	0.917	5.45 sec
1,2,7	$T = C * A^{2/7} / B^{4/7}$	0.6677	0.948	4.26 sec
3	$T = 0.66 * [A^{2/7} / B^{4/7}] * [d/D]^{0.1429}$	0.6593	0.945	4.19 sec
4,5	$T = 0.66 * [A^{2/7} / B^{4/7}] * [d/D]^{0.4138}$	0.6606	0.922	8.48 sec
6A	$T = 0.66 * [A^{2/7} / B^{4/7}] * [F/F_0]^{6.6334}$	0.6579	0.934	4.48 sec

### C. RESULTS OF COMBINED TASK 1, 2, AND 7 DATA

Since the test configurations for Tasks 1, 2, and 7 were identical except for the variance of areas and foam flow rates, the test data from these three tasks were combined and regressed against the basic modeling equation:

$$T = C * A^{2/7} / F^{4/7}$$

The empirical coefficient had a value of  $C=0.6677$  while the Sample Correlation Coefficient was  $r^2 = 0.948$  and the Standard Error of Estimate was 4.26 seconds.

A comparison with the regression results of Phase 1 for this fire configuration indicate that this study was successful in refining the model and reducing the scatter prevalent in Phase 1. In Phase 1, the empirical coefficient had a value of  $C=0.64$ , the Correlation Coefficient was 0.774, and the Standard Error was 16.95.

### D. TASK 3 RESULTS

As detailed in Section IV, Task 3 involved pool fires with simulated aircraft parts. The simulated parts were in the configuration of an annulus which consisted of a concentric ring within the outer retaining ring. Outer and inner ring size varied so as to vary the outer area to inner area ratio. The Foam Application Rate was held constant relative to these varying area ratios. The simulated parts did not have suppression blocking or thermal mass characteristics.

When Task 3 data was regressed against the basic modeling equation

$$T = C * A^{2/7} / F^{4/7}$$

the empirical coefficient was  $C=0.8239$ . The Sample Correlation Coefficient was  $r^2 = 0.958$  while the Standard Error of Estimate was 4.02 seconds. The increase in the empirical coefficient from 0.66 (Tasks 1 and 2) to 0.8239 (Task 3) indicates that the fires from Task 3 took approximately 25 percent longer to control than the fires from Tasks 1 and 2.

#### 1. Task 3 Foam Flow Model Results

This type of fire takes longer to control than a simple pool fire because the foam has to flow around the annulus rather than straight across the pool as in the simple pool fire model. The difference in control times should, therefore, be reflected in the difference in the distances for the two foam

flow paths. Figure 23 shows the foam's flow around the annulus. The distance that the foam must travel around the annulus is:

$$d = \pi * ((r_2 - r_1)/2 + r_1)$$

while D is the distance the foam would travel for a simple pool fire. The basic modeling equation was modified to

$$T = C * [A^{2/7} / F^{4/7}] * (d/D)^{0.1429}$$

where the exponent 0.1429 was determined by force-fitting the data to the following equation:

$$T = 0.66 * [A^{2/7} / F^{4/7}] * (d/D)^V$$

When the data from Task 3 were regressed against the modified model, the empirical coefficient was found to be  $C=0.6593$ . The Sample Correlation Coefficient was  $r^2 = 0.954$  and the Standard Error of Estimate was 4.19 seconds. These results indicate a strong relationship between the modified model and the Task 3 data.

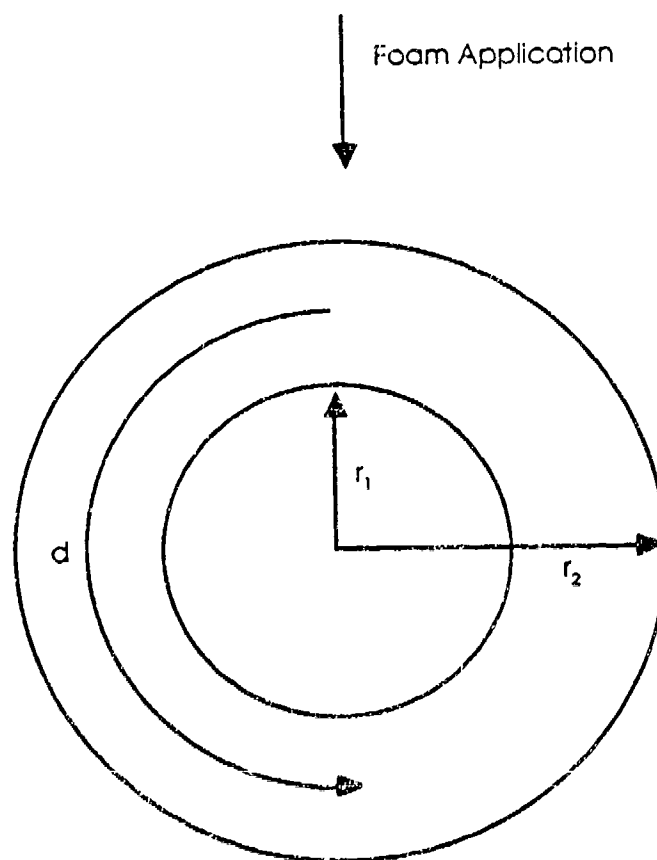
#### E. TASK 4 RESULTS

As detailed in Section II, the objectives of Task 4 included finding the relationship between Control Time, Foam Application Rate and Pool Area in the presence of simulated aircraft parts. In this Task, the simulated parts took the form of semicircular barriers of varying radius (2.18 - 5.91 feet). The barriers were 3 feet high and could block suppression efforts in certain regions of the pool. The barriers did not have any appreciable thermal mass.

When Task 4 data were regressed against the basic modeling equation

$$T = C * A^{2/7} / F^{4/7}$$

the empirical coefficient had a value of  $C=1.4048$ . The Sample Correlation Coefficient was  $r^2 = 0.920$  while the Standard Error of Estimate was 8.72 seconds. The value of the empirical coefficient,  $C=1.4048$ , indicates that this type of fire takes approximately twice as long to suppress as a basic pool fire with no obstacles.



$$d = \frac{PI * (r_2 - r_1)}{2 + r_1}$$

Figure 23. Task 3 Foam Flow Model

## F. TASK 5 RESULTS

As shown in Section II, the objective of Task 5 was to find the relationship between Control Time, Foam Application Rate, Pool Area and Preburn Time in the presence of simulated aircraft parts with suppression blocking and thermal mass characteristics. The simulated parts, identical with the simulated parts from Task 4, consisted of semicircular barriers that were 3 feet high and had a radius of 3.99 feet.

When the data from Task 5 were regressed against the basic modeling equation

$$T = C * A^{2/7} / F^{4/7}$$

the empirical coefficient was found to be  $C=1.8652$ . The Sample Correlation Coefficient was  $r^2 = 0.979$  while the Standard Error of Estimate was 4.69 seconds. The value of the empirical constant dictates that this type of fire takes approximately three times longer to suppress than a pool fire with no obstacles. From the videotapes it appears that these fires took longer to control than the Task 4, fires for two reasons: (1) in an effort to cool the barrier, it appeared that the firefighters spent more time in trying to spray foam on the barrier, rather than around it, than they did in Task 4; and, (2) there appeared to be a great deal more vaporization occurring as the foam hit the barrier than in Task 4. This would be caused by the greater amount of thermal energy stored in the Task 5 barriers. It is questionable whether the Task 5 fires would have taken longer to control if they had used the same technique as in Task 4.

### 1. AFFF Effectiveness in Preventing Reignition

As detailed in Section IV, thermocouples were placed in the barrier so that its temperature could be monitored during fire suppression efforts and after the fire had been extinguished. Because of different preburn times for each test, the maximum temperature of the barrier varied from test to test but was always several hundred degrees above the fuel autoignition temperature before suppression began. In all cases, the direct application of foam on the barrier cooled the barrier surface temperature to below the autoignition temperature of JP-4 Aviation Fuel. However, in two cases, the surface temperature increased after original suppression to values above the fuel autoignition temperature. In those tests, the AFFF successfully prevented reignition of the fuel. Table 11 summarizes the maximum temperatures reached at the different thermocouple

locations after suppression. Figure 24 is a time history of the lower barrier surface temperatures of Test 5.2. In Test 5.2, the surface temperature of the barrier at fuel level reached 460 degrees Centigrade, nearly twice the autoignition temperature of JP-4. AFFF appears to be very effective in preventing fuel reignition.

TABLE 11. MAXIMUM TEMPERATURE AT EACH LOCATION FOLLOWING SUPPRESSION.

TEST 5.2						
LOCATION	1	2	3	4	5	6
TEMPERATURE (C)	590	853	676	415	630	460
TEST 5.3						
LOCATION	1	2	3	4	5	6
TEMPERATURE (C)	365	212	161	144	91	115
TEST 5.4						
LOCATION	1	2	3	4	5	6
TEMPERATURE (C)	440	254	171	200	110	152
TEST 5.5						
LOCATION	1	2	3	4	5	6
TEMPERATURE (C)	515	436	300	225	126	167
TEST 5.6						
LOCATION	1	2	3	4	5	6
TEMPERATURE (C)	545	347	217	277	145	177
TEST 5.8						
LOCATION	1	2	3	4	5	6
TEMPERATURE (C)	367	310	305	113	102	103

LOCATION 1 - Upper surface facing firefighters.  
 LOCATION 2 - Upper surface, imbedded in the center of the plate.  
 LOCATION 3 - Upper surface facing away from firefighters.  
 LOCATION 4 - Lower surface facing firefighters.  
 LOCATION 5 - Lower surface, imbedded in the center of the plate.  
 LOCATION 6 - Lower surface facing away from firefighters.

AUTO-IGNITION TEMPERATURE (JP-4) 246 C

# Surface Temperature vs Time, Test 5.2

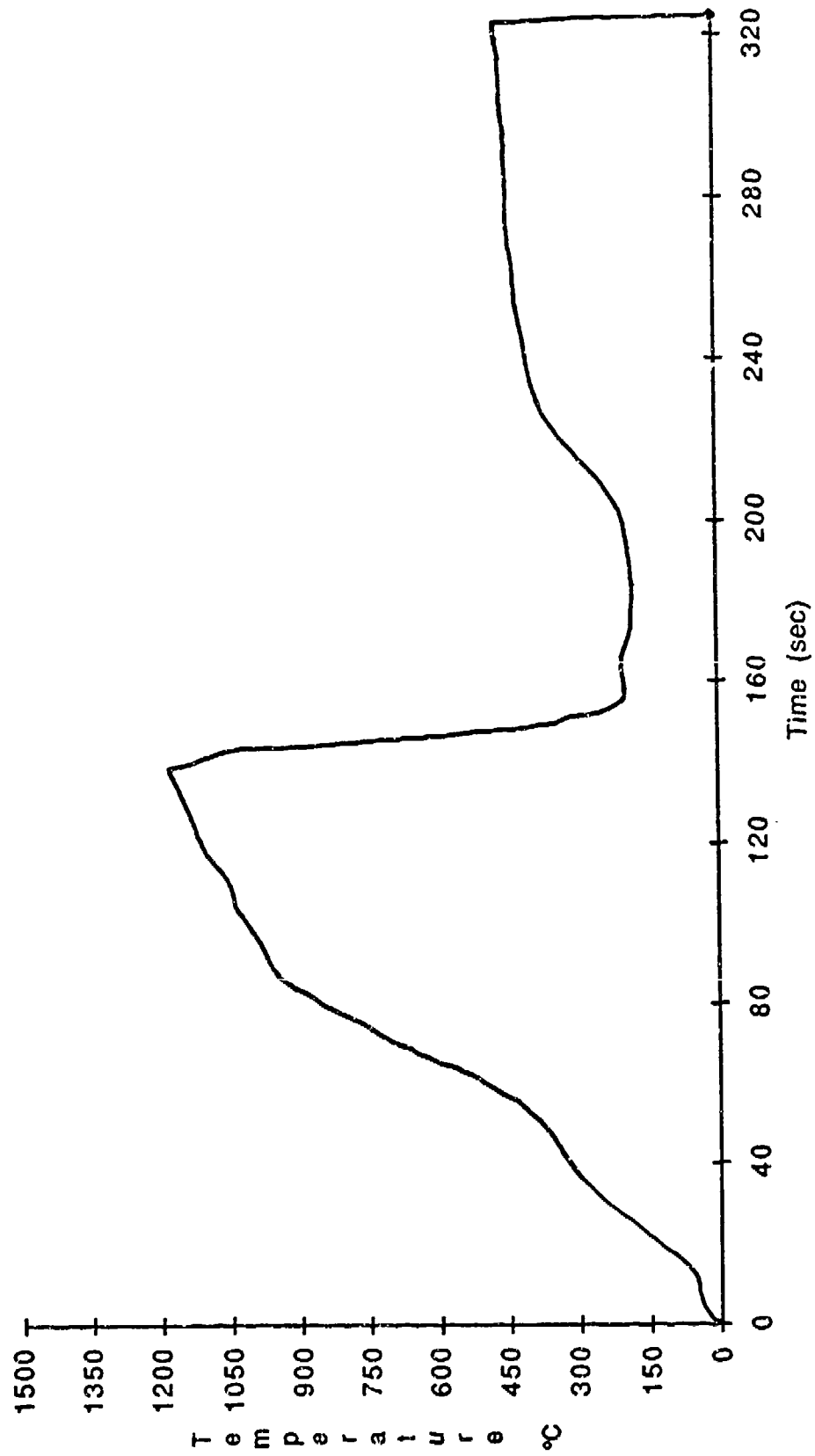


Figure 24. Obstacle Temperature Profile

## 2. Task 4 and 5 Foam Flow Model Results

Because the geometric parameters of Task 4 and Task 5 testing are identical, the data from these two Tasks were combined and regressed against a modified equation that accounted for the different foam flow paths. As in Task 3, a term was derived to describe the foam's flow around the obstacle. Figure 25 is a diagram of the foam's flow around the barrier. The distance the foam must travel around the barrier is

$$d = 3/2 * (r_2 - r_1) + \pi * ((r_2 - r_1)/2 + r_1) + r_1.$$

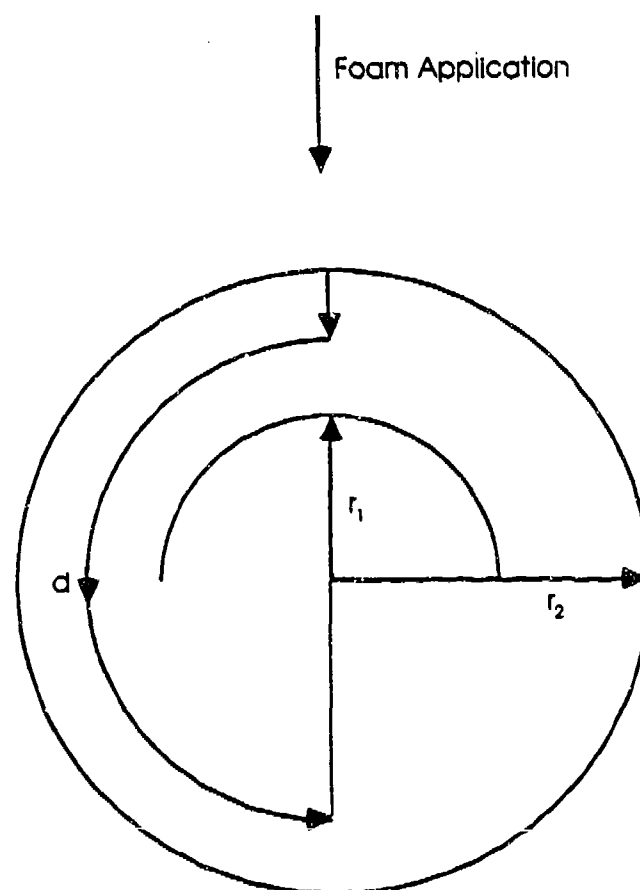
The Task 4 and 5 data were then force-fit to the following equation:

$$T = 0.66 * [A^{2/7} / F^{4/7}] * [d/D]^y$$

where d is the distance the foam must flow around the barrier and D is the diameter of the pool. The exponent, y, was found to be 0.4138. The data was then regressed against the following equation

$$T = C * [A^{2/7} / F^{4/7}] * [d/D]^{0.4138}.$$

For this model C=0.6606, while the Sample Correlation Coefficient was  $r^2 = 0.922$  and the Standard Error of Estimate was 8.48 seconds.



$$d = 3/2(r_2 - r_1) + \pi * ((r_2 - r_1) / 2 + r_1) + r_1$$

Figure 25. Task 4 and Task 5 Foam Flow Mode

## G. TASK 6A OBJECTIVE

The objective of Task 6A was to determine if the basic modeling equation was applicable to a two dimensional fire. As detailed in Section II, the relationship between Control Time, Foam Application Rate, and Pool Area for a continuously fueled expanding pool fire was sought. The steady-state pool area, A, was determined through a liquid spill model described in Section IV. After regressing the data from Task 6A against the basic modeling equation:

$$T = C * A^{2/7} / F^{4/7}$$

the empirical constant was  $C=1.657$ . The Sample Correlation Coefficient was  $r^2 = 0.934$  and the Standard Error of Estimate was 4.48 seconds. The value of the empirical constant dictates that this type of fire takes approximately 2.5 times longer to suppress than the basic one-dimensional pool fire.

### 1. Task 6A Foam Flow Model Results

One problem encountered in modelling the foam spread in a continuous source fire is that the fuel flows outwards from the center of the pool and opposes the inward flow of the foam. The gravity spread model described in Section IV was modified to account for the flow of foam on fuel and the opposition of these flows. To approximate foam flow from one edge of the pool to the other, the pool area was assumed to be in the shape of a circle sector with the radius of the sector equal to the diameter of the pool fire area. A diagram of the equivalent sector is shown in Figure 26.

For a circle sector the gravity spread model for foam on fuel with opposing fuel flow becomes:

$$F_m = \rho * V * dA * dT - M_f * dA * dT$$

where

- $F_m$  = mass flow of foam
- $\rho$  = density of foam
- $V$  = velocity of foam =  $(2 * g * dH)^{1/2}$
- $dH$  = height of foam
- $g$  = gravitational constant
- $M_f$  = mass flow of fuel
- $dA$  =  $\Theta * r^2$
- $\Theta$  = angle of sector =  $\pi/2$
- $dT$  = delta time.

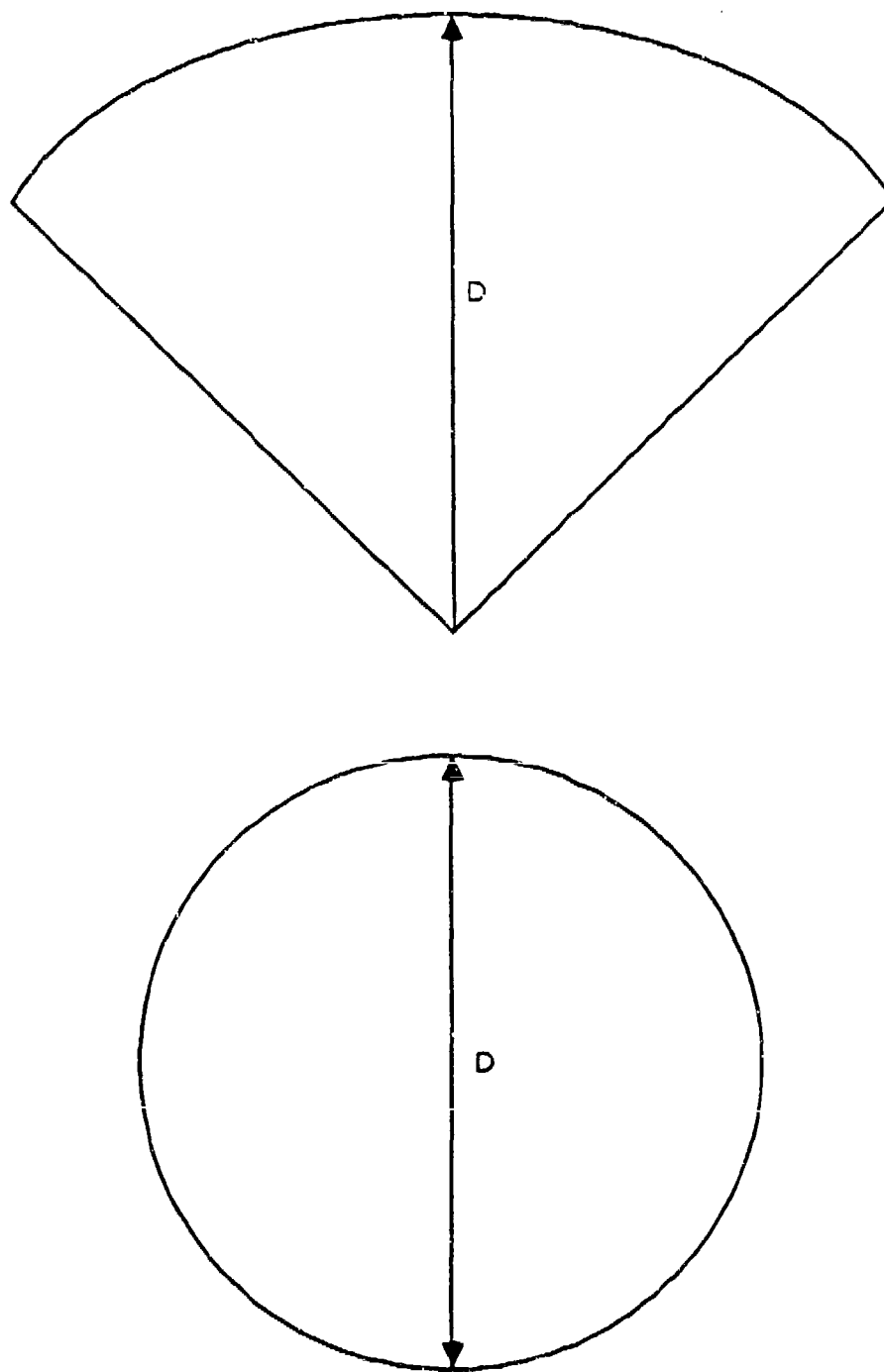


Figure 26. Equal Area Circle and Sector  
70

This equation was solved numerically with and an effective foam flow rate was calculated for the time it took for the foam to cover the pool area. Appendix A presents a graph (Figures A-1) that shows effective foam flow rates calculated for different areas and foam flow rates.

The Task 6A test data were then regressed against a modified model. This model has the form

$$T = C * [A^{2/7} / F^{4/7}] * [F/F_e]^{6.6334}$$

where  $F_e$  was the effective Foam Application Rate for a standing pool fire as calculated above and  $Q$  was the actual Foam Application Rate used in the test. The empirical coefficient had a value of  $C=0.6539$ . The Sample Correlation Coefficient was  $r^2 = 0.939$  and the Standard Error of Estimate was .00 seconds.

#### H. TASK 6B RESULTS

As discussed in the Section II, the objective of Task 6B was to investigate the applicability of the basic model when applied to a three dimensional model. In Task 6B, fuel from a continuous source was allowed to run down an inclined plane (simulated aircraft wing) and form an expanding pool fire at its base. The 10 percent criteria used to determine Control Time in previous tasks could not be used because none of the Task 6B fires were controlled to the 10 percent level. Instead of the 10 percent of maximum steady-state radiometer output used previously, a value of 25 percent was used for the Task 6B fires. The pool areas of the Task 6B fires were calculated with the fuel spill model used for Task 6A. When Task 6B data were regressed against the basic modeling equation

$$T = C * A^{2/7} / F^{4/7}$$

the empirical coefficient was found to be  $C=2.808$ . The Sample Correlation Coefficient was  $r^2 = 0.917$  while the Standard Error of Estimate was 5.45 seconds. This type of fire takes approximately 4.5 times longer to control than the simple pool fire.

Because of the gravity potential of the fuel flowing downwards and the incline of the ramp, it was impossible for the foam to completely cover the fuel on the ramp. This may explain why the fires could not be controlled to within the 10 percent criteria. This particular configuration cannot be modelled with the assumption that control time is determined by the time it takes for the foam to completely cover the pool area. For this reason no attempts were made to further modify the basic model for the Task 6B fires.

## I. COMPREHENSIVE MODEL

The objective in deriving all the modified flow models was to obtain one comprehensive model, capable of being used for all the fire configurations, except three-dimensional, encountered in this program. A model of this type would greatly simplify the task of choosing a particular model for a particular fire configuration. This model, formulated by combining all the models developed previously, has the form

$$T = 0.66 * (A^{2/7} / F^{4/7}) * (d/D)^{0.4138} * (F/F_e)^{6.6339}$$

where  $d$  = the distance the foam has to travel to completely cover the pool area with the presence of an obstacle.

$D$  = the diameter of the pool area

$F_e$  = the effective foam flow rate which takes into account the opposing flow of fuel in a two-dimensional fire.

The extension  $(d/D)$  and  $(F_e/F)$  terms are extra terms to describe obstacle fires and two-dimensional fires. For a fire without obstacles,  $d$  becomes  $D$  and the additional term becomes one. For non-two-dimensional fires,  $F_e$  becomes  $F$  and the term becomes one. The model can, thus, be used for simple pool fires, obstacle fires and two-dimensional fires.

The  $(d/D)^{0.1429}$  term of Task 3 was omitted since the  $(d/D)^{0.4138}$  term can be conservatively used for Task 3 fires. This way only one term can be used to describe all obstacle fires. For two-dimensional fires, the area can be determined through the graph in Figure 12 of Section V. There are plots of  $F_e$  vs  $F$  for different areas contained in Appendix A to facilitate use of the model.

Figure 27 is a plot of estimated vs actual control time of Task 1, 2, 3, 4, 5, 6A, and 7 data for this model.

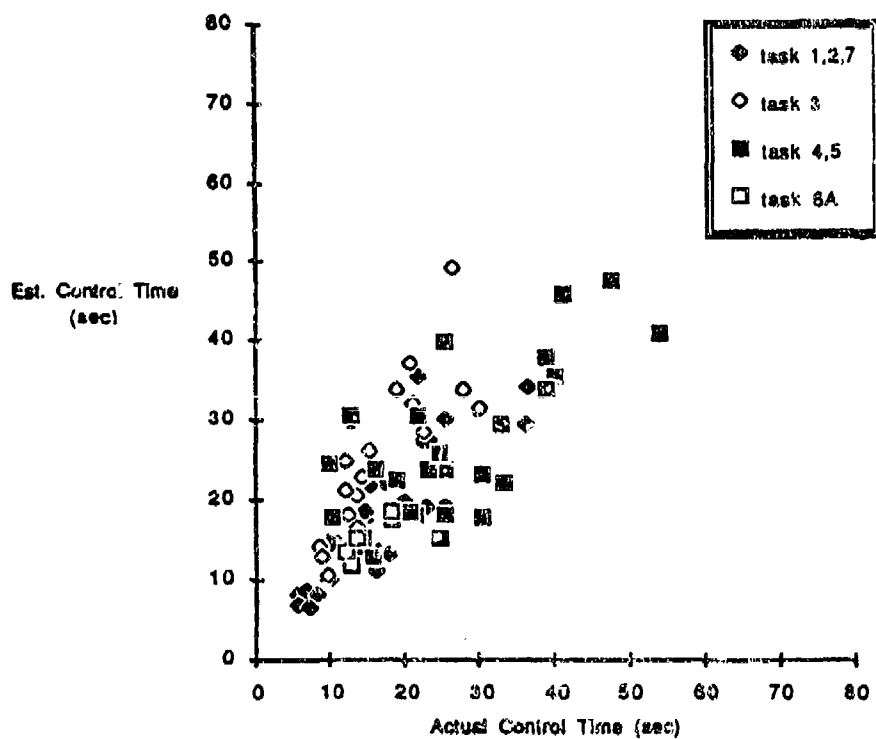


Figure 27. Estimated Control Time vs Actual Control Time

## SECTION IX

### CONCLUSIONS AND RECOMMENDATIONS

#### A. CONCLUSIONS

A statistical analysis of the data collected in this research program combined with the theoretical models which describe the spread of foam on a fuel surface, has shown the following:

1. It is feasible to correlate AFFF control of aviation fuel fires with a semitheoretical expression of the form

$$T = C * (A^{2/7} / F^{4/7})$$

where C varies with the fire configuration. C increases with the complexity of the fire configuration. For simple pool fires, the results from this study are similar to the Phase 1 results except that the standard error of the Phase 2 model is substantially lower.

2. A comprehensive model that can be used for simple pool fires, obstacle fires, and two-dimensional fires was developed:

$$T = 0.66 * (A^{2/7} / F^{4/7}) * (d/D)^{0.4138} * (F_e/F)^{0.8242}$$

where d = the distance the foam has to travel to completely cover the pool area with the presence of an obstacle

D = the diameter of the pool area

F<sub>e</sub> = an effective foam flow rate which takes into account the opposing flow of fuel in a two-dimensional fire

3. The predictive models are limited. They appear to be only effective for windspeeds less than 15 mi/hr. At windspeeds greater than 15 mi/hr, there are problems in properly applying foam to the fire. In addition, there appears to be a lower bound at which foam flow rates below this bound do not affect control time. This bound is approximately 0.10 gal/ft<sup>2</sup>-min for two-dimensional fires and 0.05 gal/ft<sup>2</sup>-min for all the other types of fires studied in this program (except three-dimensional).

use of AFFF flow rates greater than 0.15 gal/ft<sup>2</sup>-min can be considered excessive. This was found to be true for all fires except three-dimensional fires.

5. AFFF is effective in containing fuel vapor such that re-ignition does not occur when a heated object is present in the fire. In one test, the surface temperature of the object was nearly twice as high as the fuel autoignition temperature and reignition did not occur.

6. It is questionable whether AFFF is an effective method for extinguishing three-dimensional fires. None of the three-dimensional fires in this study were controlled to within 10 percent of the maximum heat flux.

## B. RECOMMENDATIONS

The model appears to be conclusive for simple pool fires. The results of this study compare favorably with those of Phase 1. For obstacle fires, more research is required to study the effects of various obstacle types on foam flow and verify whether the obstacle model developed in Phase 2 is consistent for these objects.

It appears that it is feasible to model AFFF suppression of two-dimensional models. A promising model was developed for the two-dimensional configuration, but there is not enough data to fully evaluate it. A larger data base is needed for the model to be conclusive. As for three-dimensional fires, it is possible that control may be attained with an overwhelming amount of foam with respect to the fire. The results of this study indicate that it may be questionable whether a two-dimensional agent such as AFFF is appropriate for a three-dimensional fire. More research is needed to determine whether AFFF is a viable agent in controlling three-dimensional fires.

(The Reverse Of This Page Is Blank)

APPENDIX A

EQUIVALENT FOAM FLOW RATES  
FOR TWO-DIMENSIONAL FIRES

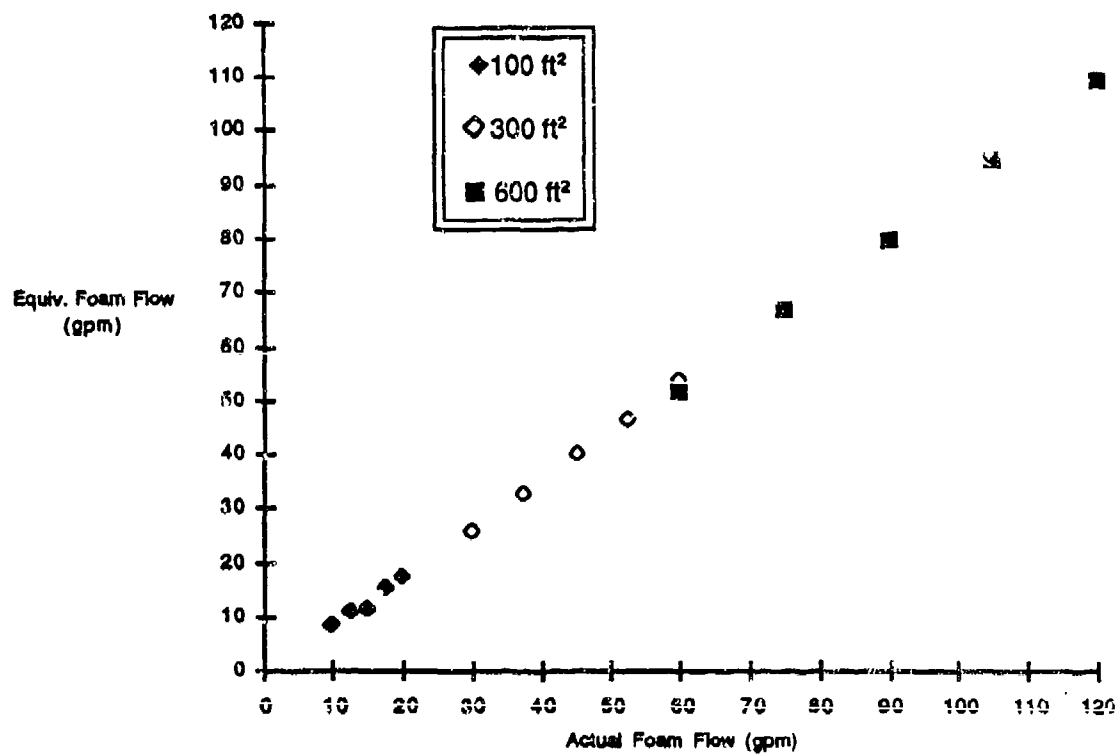


Figure A-1. Equivalent Foam Flow vs Actual Foam Flow

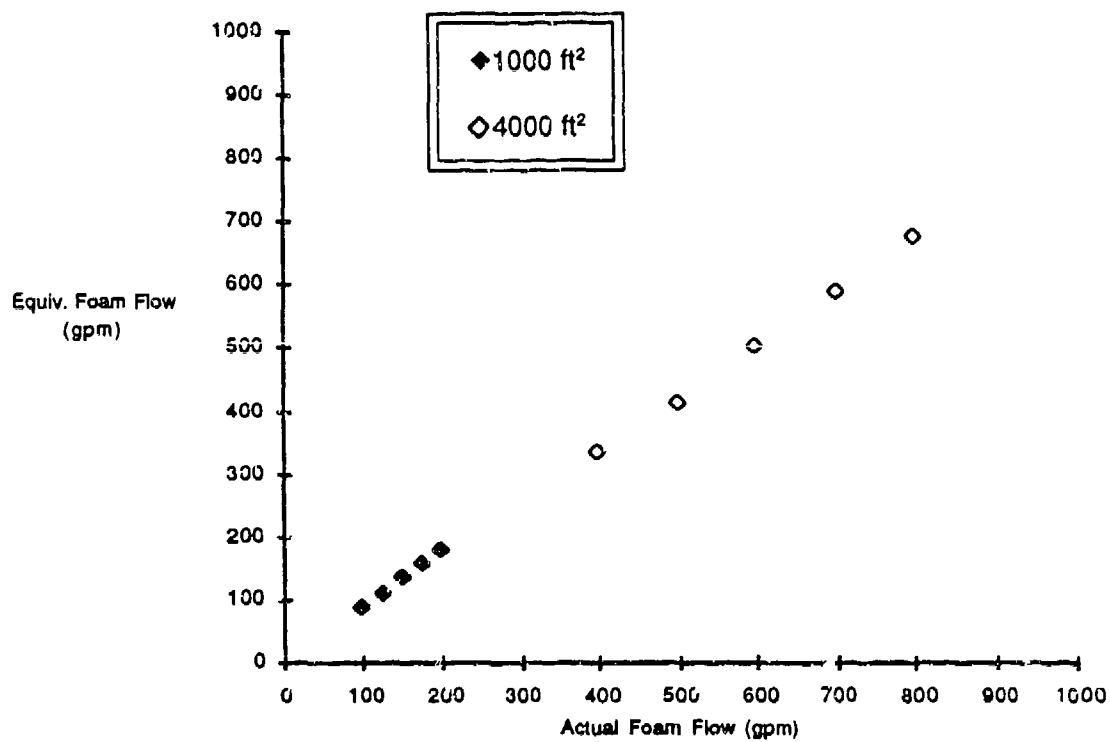


Figure A-1. Equivalent Foam Flow vs Actual Foam Flow (Concluded)